

SPECIAL ISSUE PAPER

Assessment of wildland fire impacts on watershed annual water yield: Analytical framework and case studies in the United States

Dennis W. Hallema^{1,2} | Ge Sun¹ | Peter V. Caldwell³ | Steven P. Norman⁴ | Erika C. Cohen¹ | Yongqiang Liu⁵ | Eric J. Ward⁶ | Steven G. McNulty¹

¹Eastern Forest Environmental Threat Assessment Center, Southern Research Station, U.S. Department of Agriculture Forest Service, Raleigh, North Carolina 27606, USA

²Oak Ridge Institute for Science and Education, U.S. Department of Energy, Oak Ridge, Tennessee 37830, USA

³Coweeta Hydrologic Laboratory, Southern Research Station, U.S. Department of Agriculture Forest Service, Otto, North Carolina 28763, USA

⁴Eastern Forest Environmental Threat Assessment Center, Southern Research Station, U.S. Department of Agriculture Forest Service, Asheville, North Carolina 28804, USA

⁵Center for Forest Disturbance Science, Southern Research Station, U.S. Department of Agriculture Forest Service, Athens, Georgia 30602, USA

⁶Oak Ridge National Laboratory, U.S. Department of Energy, Grand Rapids, Minnesota 55744, USA

Correspondence

Dennis W. Hallema, Eastern Forest Environmental Threat Assessment Center, Southern Research Station, U.S. Department of Agriculture Forest Service, 920 Main Campus Dr. Suite 300, Raleigh, NC 27606, USA.

Email: dwhallem@ncsu.edu

Funding information

Joint Fire Science Program, U.S. Department of Agriculture Forest Service Southern Research Station.

Abstract

More than 50% of water supplies in the conterminous United States originate on forestland or rangeland and are potentially under increasing stress as a result of larger and more severe wildfires. Little is known, however, about the long-term impacts of fire on annual water yield and the role of climate variability within this context. We here propose a framework for evaluating wildland fire impacts on streamflow that combines double-mass analysis with new methods (change point analysis, climate elasticity modeling, and process-based modeling) to distinguish between multiyear fire and climate impacts. The framework captures a wide range of fire types, watersheds characteristics, and climate conditions using streamflow data, as opposed to other approaches requiring paired watersheds. The process is illustrated with three case studies. A watershed in Arizona experienced a +266% increase in annual water yield in the 5 years after a wildfire, where +219% was attributed to wildfire and +24% to precipitation trends. In contrast, a California watershed had a lower (−64%) post-fire net water yield, comprised of enhanced flow (+38%) attributed to wildfire offset (−102%) by lower precipitation in the post-fire period. Changes in streamflow within a watershed in South Carolina had no apparent link to periods of prescribed burning but matched a very wet winter and reports of storm damage. The presented framework is unique in its ability to detect and quantify fire or other disturbances, even if the date or nature of the disturbance event is uncertain, and regardless of precipitation trends.

KEYWORDS

change point analysis, climate change, climate elasticity, hydrologic disturbance, prescribed burning, United States, wildfire

1 | INTRODUCTION

Concerns about wildfire impacts on water supply have grown in recent years as a result of longer wildfire seasons and increasing annual area burned (Neary, Ryan, & DeBano, 2005; Bladon, Emelko, Silins, & Stone, 2014). Reliable water supply is a critical ecosystem service of forests and rangelands, where more than 50% of freshwater supply in the conterminous United States (CONUS) originates (Brown, Hobbins, &

Ramirez, 2008; Sun et al., 2015a). In these areas, fire impacts on peak flows, base flows, and annual water yields can last for years and potentially affect downstream municipal water supplies (Shakesby & Doerr, 2006; Silins et al., 2014), and this is a critical issue given the increasing demand for water. Wildfire can disrupt the hydrologic cycle in several ways. The formation of an ash layer or hydrophobic layer may inhibit infiltration and reduce lateral flow in the soil (DeBano, 2000; Jung, Hogue, Rademacher, & Meixner, 2009), while evapotranspiration (ET)

can decline as a result of canopy loss. Canopy loss increases net precipitation at the surface (Helvey & Patric, 1965; National Research Council, 2008), leading to more surface runoff and accelerated storm flow. Examples are known in the western US of increases in storm runoff between 9% and 88% (Jung et al., 2009), and annual yield increases in the first post-fire year between 50% and 200% (Helvey, 1980; Troendle & Bevenger, 1996; Bart, 2016); however, these effects vary by geographic region and depend on pre-fire conditions, fire severity, and post-fire climate (Neary et al., 2005). ET may decline for several months even after a low severity prescribed fire (Clark, Skowronski, Gallagher, Renninger, & Schäfer, 2012; Renniger, Clark, Skowronski, & Schäfer, 2013). Given the importance of ET for the water balance (Sun et al., 2015a, 2015b), this may alter streamflow response depending on local conditions. Yet in absence of any widely applicable approach to link streamflow variations to fire disturbance, impacts on streamflow remain largely unquantified across broad regions.

Paired watershed analysis has long been the standard for quantifying multiyear disturbance impacts (Bosch & Hewlett, 1982); however, a lack of comparable conditions between watersheds often limits the analysis to local data. Double-mass analysis (Merriam, 1937; Searcy & Hardison, 1960) requires only local data and assumes an approximately linear relationship between, for example, precipitation and streamflow when there are no changes in climate, land cover, or water withdrawals and has been used to assess streamflow changes after fire (e.g., Anderson, 1955), forest harvesting, mountain pine beetle infestations (Wei & Zhang, 2010; Zhang & Wei, 2012), and urbanization (Hao et al., 2015). The assumption of linearity represents a limitation of double-mass analysis because when gradual disturbances overlap, it is difficult to identify the undisturbed state of a system (Glenn-Lewin, Peet, & Veblen, 1992; Temperli, Bugmann, & Elkin, 2013). Time series analysis now features methods such as change point analysis (Hawkins, Qiu, & Kang, 2003; Hawkins & Zamba, 2005; Wang, Chen, & Yu, 2016) to identify the timing of significant change in the location and scale of a time series rather than relying on a second variable like the double-mass analysis and has been applied in various climate and hydrological studies (Yang, Chen, Xu, & Zhang, 2009; Huang, Xia, Guo, & Yang, 2014; Matsuyama, Marengo, Obregon, & Nobre, 2002; Vivès & Jones, 2005; Caldwell et al., 2016). The simultaneous effect of climate variability on streamflow can be filtered with a climate elasticity model (CEM; Schaake, 1990; Sankarasubramanian, Vogel, & Limbrunner, 2001) that expresses the rate of streamflow change as the rate of change of a set of climate parameters, such as precipitation and temperature (Fu, Charles, & Chiew, 2007) or precipitation and potential evapotranspiration (PET) (Hao et al., 2015). Biederman et al. (2015) found that the CEM with precipitation and temperature parameters was not a significantly better model than the CEM based on precipitation alone.

Despite the large number of studies conducted in California, the Southwestern United States, the Rocky Mountains, and the Southeastern United States, current knowledge about fire impacts on annual water yields in the United States is fragmentary and based primarily on only a small number of experimental watersheds in the western states. The restricted set of fire properties, watershed characteristics, and climate patterns in these watersheds limits the understanding of the broader range of possible relationships and effects, and the question then is (1) how to adequately combine hydrological data and

methods in order to detect impacts of local fires on water yields at the watershed scale and (2) how to distinguish these fire impacts from the effects of other watershed disturbances.

1.1 | Objectives and approach

The objective of this study was to develop and demonstrate a general framework for the assessment of wildland fire impacts (wildfire and prescribed fire) on watershed annual water yields by separating the effects of local fires from the effects of climate variability and other watershed disturbances. This framework responds to the need to incorporate wildland fire effects into the assessment of water supplies in order to adapt planning efforts to the resilience of local water supplies to fire impacts (Martin, 2016) and answers to calls for a useful tool of fire impact assessment in addition to existing pyrogeographic frameworks (Bowman, O'Brien, & Goldammer, 2013; Krawchuk & Moritz, 2014). It relies only on local climate and streamflow data, using pre-disturbance and post-disturbance streamflow data as opposed to alternative approaches relying on watershed pairs, and combines the classical techniques of double-mass and flow duration analysis with recent techniques including change point analysis, climate elasticity modeling, and process-based hydrological modeling. A non-exhaustive demonstration of this framework includes three case studies on watersheds in three different physiographical regions of the CONUS, that is, South Carolina (with annual prescribed burning), Arizona, and California (both with wildfires). Special consideration was given to the South Carolina watershed, where we used the change point model to detect and characterize multiple types of disturbance in the streamflow data.

2 | METHODS

2.1 | Framework for evaluating wildland fire impacts on streamflow

The framework for evaluating the impacts of hydrologic disturbance in watersheds consists of five methods that address various aspects of hydrological changes and disturbances evaluated for a multiyear post-disturbance period with respect to a reference period.

1. Determining the timing of hydrologic disturbance with the change point model (CPM)
2. Double-mass analysis of streamflow and precipitation data (DMC)
3. Analysis of precipitation duration curves (PDC) and streamflow duration curves (FDC)
4. Attribution of changes in streamflow to climate variability and watershed disturbance using the climate elasticity model (CEM)
5. Comparison with attribution analysis obtained from results of the process-based Water Supply Stress Index model (WaSSI)

2.1.1 | Timing the hydrologic disturbance with the change point model

The CPM (Hawkins et al., 2003; Hawkins & Zamba, 2005) can detect change points in a continuous time series corresponding with an

unidentified disturbance such as wildland fire. An undisturbed continuous time series of streamflow may be assumed to follow a single distribution F_0 ; however, if a change point exists, the time series will follow a distribution F_1 prior to the change point and a distribution F_2 after the change point, where $F_1 \neq F_2$. Consequently, we defined the null hypothesis for a streamflow series without change points as follows (after Hawkins & Zamba, 2005; Ross, 2015):

$$H_0 : Q_i \sim F_0(Q; \theta_0) \quad i = 1, 2, \dots, T \quad (1)$$

where discharge Q at any given moment i follows one single distribution F_0 , which is a function of Q and a set of parameters θ_0 . The alternative hypothesis was defined as follows:

$$H_1 : Q_i \sim \begin{cases} F_1(Q; \theta_1) & i = 1, 2, \dots, \tau \\ F_2(Q; \theta_2) & i = \tau + 1, \tau + 2, \dots, T \end{cases} \quad (2)$$

where Q_i follows distribution F_1 defined by parameter set θ_1 prior to change point τ and distribution F_2 afterwards with a different set of parameters θ_2 .

The null hypothesis was tested by running through the entire time series and calculating the non-parametric two-sample Lepage (L) statistic at each time step and evaluating the differences between the parts of the time series before and after every potential τ . Lepage combines the Mann-Whitney (or Wilcoxon rank sum) statistic (denoted U) for detecting location shifts with the Mood statistic for detecting scale (dispersion) shifts (denoted M , Lepage, 1971):

$$L = U^2 + M^2. \quad (3)$$

Refer to the Appendix for the formulations of U and M . A change in streamflow was detected when L exceeded a critical value h_t corresponding with a given significance level ($\alpha = 0.05$) total sample size n . Lepage-type tests do not require any knowledge of the underlying distribution of observations and provide greater statistical power than the Mann-Whitney, Chi-square and student's t -test statistics (Hirakawa, 1974; Lloyd, Freer, Collins, Johns, & Jones, 2014). Applications include the detection of abrupt changes in precipitation (Matsuyama et al., 2002; Vivès & Jones, 2005), sunshine rate (Inoue & Matsumoto, 2007), streamflow (Yang et al., 2009), and the evaluation of the impact of reservoirs (Huang et al., 2014). Calculations were performed using the *cpm* software in R (Ross, Tasoulis, & Adams, 2011; Ross, 2015; R Core Team, 2014).

2.1.2 | Double-mass analysis of the precipitation-streamflow relationship (DMC)

Double-mass curves (DMCs) were calculated using the monthly Parameter-elevation Regressions on Independent Slopes Model (PRISM) precipitation and United States Geologic Survey (USGS) streamflow data to confirm the existence of a break point in the precipitation-streamflow relationship indicating a change in water yields. First, two linear models (the unrestricted models) were fitted to the reference and post-disturbance periods separately and one linear model (the restricted model) was fitted to the pooled data for both periods. Subsequently, a Chow test was performed to evaluate the equality of model coefficients of the unrestricted models versus the restricted model. Monthly data were used to allow a more precise

separation of reference and post-disturbance data, which was necessary given a variable seasonal timing of disturbance events in different watersheds. See Appendix for equations.

2.1.3 | Characterization of changes in precipitation duration and flow duration (precipitation duration curve and flow duration curve)

In order to characterize and visualize changes in the time distribution of precipitation and streamflow between the reference and post-disturbance period, we calculated the reference and post-disturbance PDCs and FDCs for each watershed according to the flow duration principle (Foster, 1934; Vogel & Fennessey, 1994; see Appendix). Precipitation duration curves were calculated from Daymet precipitation aggregated to the watershed scale, and flow duration curves were calculated from the USGS GAGES-II daily streamflow data. We then identified changes in the number of precipitation days (or "rain" days) > 1 mm and the number of extreme precipitation days with ≥ 50.8 mm (Karl, Knight, & Plummer, 1995).

2.1.4 | Attribution of changes in streamflow to climate variability and watershed disturbance using the climate elasticity model

The CEM was used to identify the portion of change in mean annual streamflow attributed to climate variability as opposed to the change caused by a disturbance. We calculated for each watershed a reduced one-parameter model (CEM_0) and a two-parameter model (CEM_1). The one-parameter model was formulated as (Schaake, 1990; Sankarasubramaniam et al., 2001)

$$CEM_0 : \quad \frac{dQ}{Q_0} = \alpha \frac{dP}{P_0} \quad (4)$$

and the two-parameter model as

$$CEM_1 : \quad \frac{dQ}{Q_0} = \alpha \frac{dP}{P_0} + \beta \frac{dPET}{PET_0} \quad (5)$$

where the change in mean annual streamflow as a fraction of mean annual streamflow during the reference period dQ/Q_0 is a linear function of the relative changes in mean annual precipitation dP/P_0 and potential evapotranspiration $dPET/PET_0$. Parameters α and β were fitted to the data of the reference (pre-disturbance) period.

In order to derive the contribution of watershed disturbance, or more specifically fire disturbance in the case of the AZ and CA watersheds, we assume that the observed change in streamflow (ΔQ) is comprised of a climate induced change (ΔQ_{clim}) and a component attributed to the hydrologic disturbance (ΔQ_{dist}) (Wei & Zhang, 2010; Hao et al., 2015):

$$\Delta Q = \Delta Q_{clim} + \Delta Q_{dist} \quad (6)$$

Next, the one-parameter and two-parameter CEMs of change in streamflow were evaluated with the corrected (small sample) Akaike's information criterion (AIC_c) (Sugiura, 1978; Hurvich & Tsai, 1991; definition given in the Appendix).

2.1.5 | Process-based attribution of streamflow changes with the Water Supply Stress Index (WaSSI) model

The process-based Water Supply Stress Index (WaSSI) was calculated to corroborate the results of the attribution analysis obtained with the empirical CEM. WaSSI (Sun, McNulty, Moore-Myers, & Cohen, 2008; Sun et al., 2011) has been used in CONUS-wide studies, for example, to evaluate environmental change impacts on ecosystem services (Caldwell, Sun, McNulty, Cohen, & Moore Myers, 2011), effects of urbanization and water withdrawals on streamflow (Caldwell, Sun, McNulty, Cohen, & Moore Myers, 2012), impacts of dairy production on water scarcity (Matlock et al., 2013), and drought effects in national forests (Sun et al., 2015a). Monthly precipitation and air temperature from gridded PRISM data were scaled to the 12-digit HUC watershed scale and used as input for WaSSI to calculate monthly water balances for eight land cover classes for the reference and post-disturbance period. Water yield simulations in WaSSI provided a baseline accounting for climate variability, and a comparison with observed streamflow allowed us to estimate the non-climate or disturbance contribution as a function of time (Equation 6). A difference with the CEM approach is that this method uses monthly time intervals instead of the reference and post-disturbance period totals. Processes simulated in WaSSI

include infiltration, ET, surface runoff, snow accumulation and snow melt, soil water storage, and streamflow. Infiltration, soil storage, and surface runoff were computed with algorithms from the Sacramento Soil Moisture Accounting Model (Burnash, Ferral, & McGuire, 1973; Burnash, 1995) with input from the State Soil Geographic Database (STATSGO; Natural Resources Conservation Service, 2012) and 2005 domestic water usage data (USGS; Kenny & Juracek, 2012). A complete description of the WaSSI model can be found in Sun et al. (2008, 2011) and Caldwell et al. (2012).

2.1.6 | Navigating the framework

The methods described above were integrated into one framework for evaluating the impacts of hydrologic disturbance in watersheds (Figure 1). There are multiple routes to navigate the framework, depending on available data and the nature of these data for a given watershed. For watersheds with a single fire disturbance in the evaluated period, the ignition date (if known) can be used to separate the reference and post-disturbance periods and no CPM is needed. The procedure for watersheds with multiple disturbances of any type (wildfire, active prescribed burning policy, logging operations, storm damage, construction, water management, or water use) relies on a

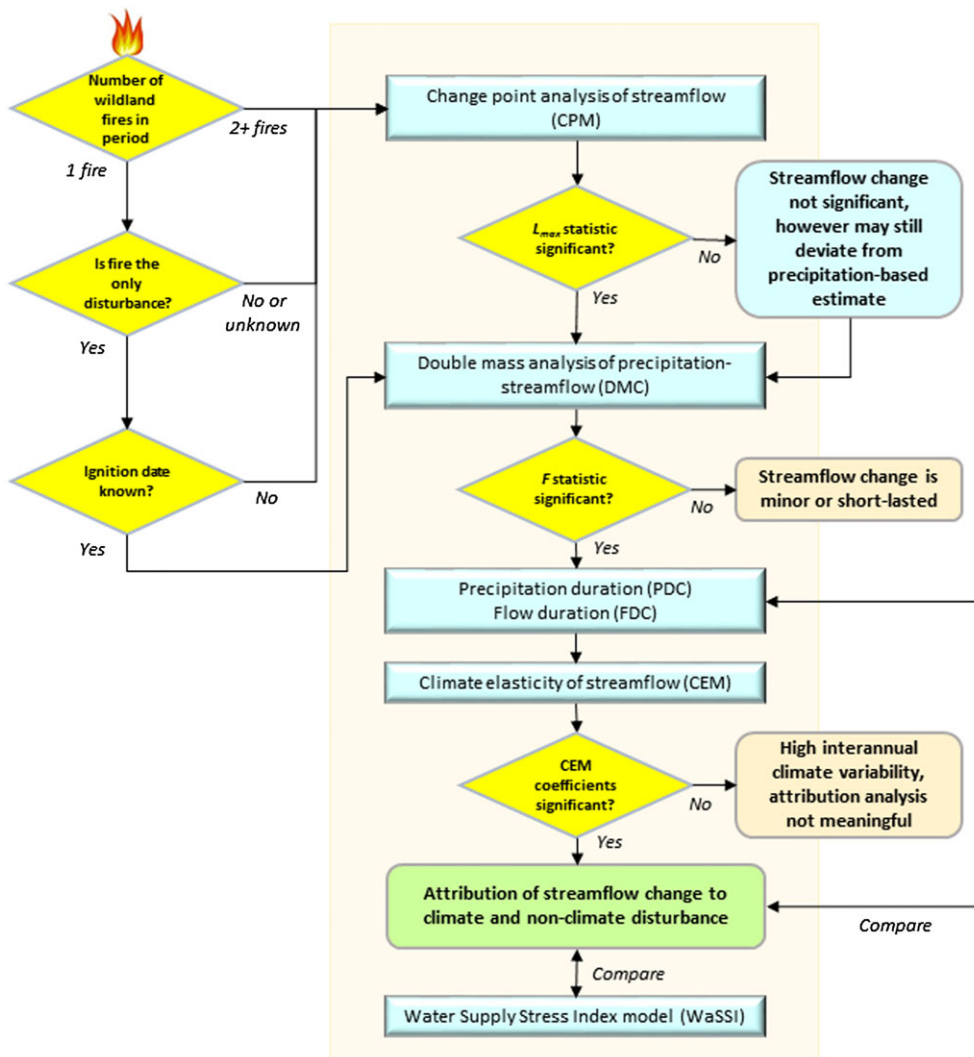


FIGURE 1 Framework for evaluating wildland fire effects on streamflow

CPM of the streamflow time series to find the timing of the disturbance event(s) with the greatest hydrologic impact. A single abrupt change in streamflow over a given time will yield a single significant maximum value L_{max} in which case the corresponding time separates the reference and post-disturbance periods. Conversely, if there is no significant L_{max} , there is no significant change in streamflow. Regardless, streamflow may still exceed the discharge predicted based on precipitation, which can be tested using the Chow test of differences in the double mass relationship between multiyear streamflow and precipitation. If the corresponding F statistic is not significant, the post-disturbance change in streamflow is minor or short-lived with regard to the length of the evaluated period, in which case the attribution analysis is not meaningful. Conversely, if the corresponding F statistic is significant, there is likely a non-climate contribution to changes in streamflow, which can be calculated with the CEM and corroborated with results from the WaSSI simulation. The PDC and FDC help to characterize changes in extreme precipitation and streamflow that may contribute to long-term changes in water supply. The normal calendar year is used for the analyses based on annual data, with the year in which the disturbance occurred included in the post-disturbance period.

2.2 | Datasets

2.2.1 | Streamflow data

An overview of all used datasets is given in Table 1. Daily streamflow data were retrieved for the flow stations 2130900 (SC), 9508300 (AZ), and 11274630 (CA), and after extracting the data for selected watersheds, daily values were aggregated to monthly and annual watershed yields. Watershed boundaries were determined using the GMTED2010 elevation model (236 × 236 m resolution).

2.2.2 | Climate data

Monthly climate precipitation was obtained from the PRISM gridded dataset (Spatial Climate Analysis Service, 2004) and scaled to the watersheds for the purpose of subsequent analysis in the change point analysis, double-mass analysis, attribution analysis, and hydrologic simulations. Daily precipitation was extracted from the gridded Daymet dataset (Thornton et al., 2014) and scaled for the precipitation and flow duration analysis. Monthly PET was calculated using Hamon's method as a function of monthly aggregated (mean) air temperature and day length (Hamon, 1961; Sun et al., 2011).

2.2.3 | Fire data and vegetation index

The Monitoring Trends in Burn Severity dataset (MTBS; Eidenshink et al., 2007) integrates fire data from across the CONUS from 1984 to present. MTBS characterizes burn severity (30 × 30 m cells) of an area within fire perimeters based on the differenced normalized burn ratio (dNBR; Key & Benson, 2006) and the relative differenced normalized burn ratio (RdNBR; Miller & Thode, 2007), which are calculated from Landsat Thematic Mapper (TM) and Enhanced Thematic Mapper (ETM+) images using the reflectance in near-infrared (Landsat band 4) and mid-infrared (Landsat band 4) recorded before and after a fire. These data have been used to analyze wildfire trends (Dennison, Brewer, Arnold, & Moritz, 2014) and forest disturbance (Hart, Schoennagel, Veblen, & Chapman, 2015) among others. MTBS data

were used to characterize the burn severity within the watersheds, after which we determined the temporal evolution of MODIS normalized difference vegetation index (NDVI) for each burn severity class in percentage.

2.3 | Study watersheds

We selected three burned watersheds in different regions of the CONUS, each with a significant burned area to drainage area ratio (>5%) and a minimum drainage area of 25 km², to demonstrate the proposed framework (Figure 2, Table 2).

2.3.1 | Black Creek watershed, South Carolina with prescribed burning (34.51°N, 80.18°W)

The Black Creek watershed (henceforward referred to as the SC watershed) is part of the greater Lower Pee Dee subbasin and the largest of the three watersheds by area (295.4 km²). It also has the lowest altitude (79–219 m) and smallest mean gradient (2.5%) and consists of grassland (21%), evergreen forest (33%, mostly longleaf pine), and deciduous forest (10%; Figure 3a). Woody wetlands are found along the Black Creek and its tributaries. The 30-year average precipitation (1981–2010) was 1,144 mm, and PET was 981 mm. Climate was characterized as temperate without dry season and with hot summers, or Cfa (Godfrey, 1999; Kottek, Grieser, Beck, Rudolf, & Rubel, 2006). Annual prescribed burning has been conducted in the Carolina Sandhills National Wildlife Refuge (NWR) in the lower portion of this mixed land use watershed since at least the 1940s, and 40% of the watershed was burned between 2004 and 2014 (Figure 3a). Burn severity was typically low. Fire impact on the interannual variability of vegetative phenology evidenced by the NDVI was limited, with seasonal NDVI values peaking between 73% and 74% and minimum values between 54% and 57% (Figure 4a).

2.3.2 | Wet Bottom Creek watershed, Arizona, and 2004 Willow wildfire (34.16°N, 111.69°W)

The Wet Bottom Creek watershed (or AZ watershed) drains 93.0 km² and has the greatest variations in terrain of the three watersheds, with slopes ranging between 0.1% and 76.1%. The upper parts with an altitude up to 2,157 m received snowfall during some winters and were covered with evergreen forest (57%) of pinyon juniper and ponderosa pine (Figure 3b). These upper parts drain through a narrow rocky valley vegetated with shrubs (43%, mostly chaparral). The climate is temperate with dry and hot summers (Csa; Godfrey, 1999) with an annual precipitation of 473 mm; however, the lower part in the western extremity of the watershed is drier. The average PET of 873 mm exceeded precipitation. The Wet Bottom Creek is a tributary of the Verde River, one of the last free-flowing perennial rivers in Arizona. Groundwater pumping in parts of the Verde River basin has raised concern about the effects on riparian vegetation (Leake & Pool, 2010). The Willow wildfire that started on June 24, 2004 affected 83.6% of the watershed, with under/unburned to low burn severity (10.7% and 46.3%, respectively, of the watershed) on the more sparsely vegetated south-facing slopes and moderate burn severity (26.2% of the watershed) on the north-facing slopes (Figure 3b). Approximately 0.5% of the watershed was affected by high severity burning. Fire reduced NDVI from

TABLE 1 Description of datasets used in the analysis

Dataset	Description	Format	Coverage/scale	Time range/scale	Updated	Source	Reference
NLCD 2001	National Land Cover Database	Spatial raster	National 30 × 30-m cells	2001	2011	Multi-Resolution Land Characteristics Consortium	Homer et al. (2015) http://www.mrlc.gov/nlcd2011.php
MTBS burned area	Monitoring trends in burn severity	Vector polygon	CONUS	1984–2014	9/25/2014	USDA Forest Service RSAC/USGS EROS	Eidenshink et al. (2007) http://www.mtbs.gov
MTBS burn severity mosaic	Monitoring trends in burn severity	Spatial raster series	CONUS, 30 × 30-m cells	1984–2014, annual	9/25/2014	USDA Forest Service RSAC/USGS EROS	Eidenshink et al. (2007) http://www.mtbs.gov
GAGES-II	Streamflow	Point time series	National	1900-present, daily	2015	USGS	USGS (2015) http://waterdata.usgs.gov/nwis
GMTED2010	Elevation model	Spatial raster	Global, 236 × 236-m cells	2010	2010	USGS	Danielson and Gesch (2011) http://topotools.cr.usgs.gov/gmted_viewer/
Daymet	Climate model	Spatial raster series	North America, 1 × 1 km	1980–2014, daily	2013	ORNL DAAC	Thornton et al. (2014)
PRISM	Elevation based climate model	Spatial raster series	CONUS, 4 × 4-km cells	1895–2014, monthly	2013	PRISM Climate Group, Oregon State University	Daly, Neilson, and Phillips (1994) Daly, Gibson, Taylor, Johnson, and Pasteris (2002) http://www.prism.oregonstate.edu/
MODIS NDVI	Vegetation index	Spatial raster series	Global 250 × 250-m cells	2000–2013, 16-day intervals	2015	NASA/USGS	http://modis.gsfc.nasa.gov/

CONUS, conterminous United States; MTBS, Monitoring Trends in Burn Severity dataset; NASA, National Aeronautics and Space Administration; NDVI, normalized difference vegetation index; NCLD, National Land Cover Database; PRISM, Parameter-elevation Regressions on Independent Slopes Model; USGS, United States Geologic Survey.

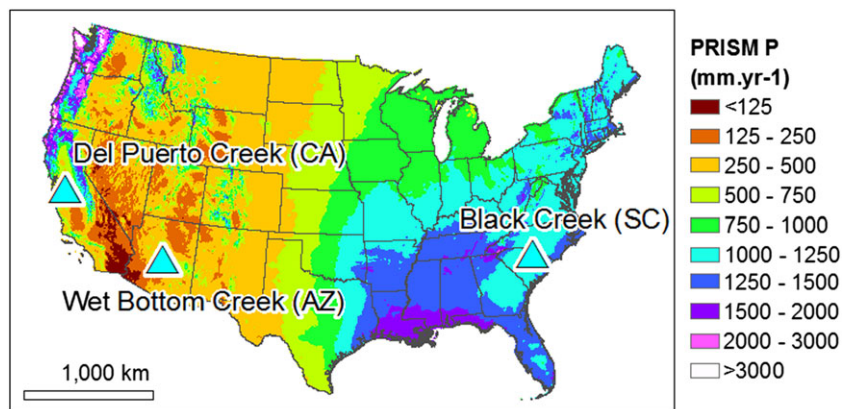


FIGURE 2 Locations of the Black Creek (SC), Wet Bottom Creek (AZ), and Del Puerto Creek (CA) watersheds within the United States, and mean annual precipitation for the period 1981–2010 (PRISM)

approximately 0.60 to 0.26 (moderate and high burn severity) and from 0.41 to 0.29 (low burn severity). After 2 years, NDVI showed signs of initial recovery in the severely affected evergreen forest (Figure 4b), and in 2014, 10 years after the fire, summer peak NDVI was 0.48 and demonstrated progress in post-disturbance recovery despite a low precipitation of <400 mm in 2006, 2009, 2011, and 2012.

2.3.3 | Del Puerto Creek watershed, California, and 2003 Deer Park wildfire (37.48°N, 121.20°W)

The Del Puerto Creek watershed (hereafter CA) spans 187.4 km² and drains into the agricultural Central Valley. Average annual precipitation was a mere 418 mm, and PET was 904 mm. The upper part of the CA watershed consisted of scrubland/shrubland with sagebrush and chaparral (57% of the watershed; Figure 3c). Overall, the CA watershed had the lowest forest cover of the three watersheds. Before disturbance, the east-facing headwater slopes had a mixed forest cover (14%, canopy cover 25–50%) with pine oak and eucalyptus and the lower eastern part of the watershed was mostly grassland (28%). The Deer Park wildfire started on July 20, 2003 on a hillslope in the upper part of the watershed and burned 14.1% of its area (Figure 3c), with moderate to high burn severity (3.8% and 1.2%, respectively, of the watershed) on the chaparral covered hillslopes and unburned/underburned to low burn severity near streams (4.9% and 4.1%, respectively). The NDVI in the severely burned area decreased (Figure 4c) from around 0.58 during the summer peak to around 0.30 in autumn. Areas categorized as unburned to underburned likewise decreased in NDVI during the same period, from approximately 0.55 to 0.33.

3 | RESULTS

We identified the 5-year reference (pre-disturbance) and 5-year post-disturbance periods immediately preceding and following the wildfire starting dates reported in the MTBS dataset for the AZ and CA watersheds, respectively. Due to the large number of prescribed fires reported for the SC watershed (44 between 1984 and 2013; MTBS), we here used the change point model to identify the most significant disturbance in the streamflow data for the period overlapping with the MTBS and PRISM datasets (1984–2012). The remainder of the analysis was performed according to the framework and included the

evaluation of DMC, PDCs and FDCs (discussed in the Appendix), CEMs, and WaSSI hydrologic simulations. Evaluated periods follow the calendar year, chosen as a trade-off between the hydrologic year, often starting on October 1 in the CONUS and the fire season, which can start as early as March or April. The AZ watershed had the greatest increase in 5-year post-wildfire annual water yield (+266%), while the SC and CA watersheds had a lower post-wildfire annual water yield (–39% and –64%, respectively).

3.1 | South Carolina watershed

3.1.1 | Change point analysis of streamflow data

Critical value h_n was exceeded in the years 1998 through 2000 using an annual time step (Figure 5a). Greater statistical power was obtained at a monthly time step (Figure 5b), which also allowed us to select the month with the greatest L (May 1999) as the disturbance change point to be evaluated.

3.1.2 | Double-mass curves

The disturbance of May 1999 also represents a break point in the relationship between cumulative streamflow and precipitation ($p < 10^{-6}$) (Figure 6a), with the coefficient of the unrestricted linear model (runoff coefficient) declining from 0.419 (5 year reference) to 0.306 in the post-disturbance period. The corresponding residual plot offers a more detailed view of the seasonal oscillations representing the time lag between cumulative precipitation and runoff caused by higher runoff in the winter, when soils are wetter than in the summer. Even compared with the 10-year reference period, the change in runoff is still significant ($p < 10^{-6}$).

3.1.3 | Attribution of streamflow change (climate elasticity model)

The one-parameter (precipitation) CEM₀ was retained at the expense of the two-parameter (precipitation and PET) CEM₁ for all three watersheds and evaluated periods (Table 3), based on a higher AIC_c value. Each CEM₁ with a positive fitted value of β was rejected because this wrongly implies a scenario where a higher PET leads to more streamflow. The 5-year CEM₀ predicted a –242-mm (–47%) change in annual streamflow versus a –201-mm (–39%) observed change (Table 3 and Figure 7a). The difference between observed

TABLE 2 Location, vegetation, hydrologic characteristics, and fire characteristics of the three study watersheds

	Black Creek, South Carolina (SC)	Wet Bottom Creek, Arizona (AZ)	Del Puerto Creek, California (CA)
Location	Carolina Sandhills NWR	Tonto National Forest	Diablo Range, Stanislaus County
USGS gauging station ID	2130900 (non-reference)	9508300 (reference)	11274630 (reference)
Physiography			
Drainage area (km ²)	295.4	93.0	187.4
Altitude (m)	79–219	715–2157	75–1113
Slope (range) (%)	2.5 (9.1)	20.1 (76.0)	19.4 (54.3)
Vegetation			
Pre-disturbance land cover and canopy cover (NLCD 2001)	Evergreen Forest (33%, canopy cover 50–75%) Grassland/Herbaceous (21%)	Evergreen Forest (57%, canopy cover >25%)	Shrub/Scrub (57%) Grassland/Herbaceous (28%) Mixed Forest (14%, canopy cover 25–50%)
	Woody Wetlands (11%, canopy cover >50% and >75%) Deciduous Forest (10%, canopy cover 50–75%)	Shrub/Scrub (43%)	
Vegetation species	Longleaf pine	Pinyon juniper, ponderosa pine, chaparral	Sagebrush, chaparral, pine oak, eucalyptus
Ecosection (province)	Southern Appalachian Piedmont (Southeastern Mixed Forest)	Tonto Transition (Colorado Plateau Semi-Desert)	Central California Coast Ranges (California Coastal Range Open Woodland-Shrub-Coniferous Forest-Meadow)
Climate (1981–2010)			
Annual precipitation (snow water equivalent) (mm)	1144 (29)	473 (126)	418 (21)
Annual PET (mm)	981	873	904
Annual water yield (mm)	379 (33%)	112 (24%)	41 (10%)
Climate classification 1961–1990 (Godfrey, 1999)	Cfa (humid subtropical)	Csa (Mediterranean with hot summers)	Csa (Mediterranean with hot summers)
Fire characteristics (MTBS)			
Name	Prescribed burning (Rx)	2004 Willow Wildfire	2003 Deer Park Wildfire
Start date	Annually from March	6/24/2004	7/20/2003
Burn severity	Low	Low to moderate	Moderate to high
Burned area to watershed area ratios	7.1% (2004) 40% (2004–2013)	83.6% (this fire) 75% (1984–2013)	14.1% (this fire) 30% (1984–2013)
(1) Under/Unburned to Low	1.4% (2004)	10.7%	4.9%
(2) Low Burn Severity	4.0% (2004)	46.3%	4.1%
(3) Moderate Burn Severity	1.7% (2004)	26.2%	3.8%
(4) High Burn Severity	0% (2004)	0.5%	1.2%

change in streamflow ΔQ_0 and the contribution of climate $\Delta -Q_{clim}$ predicted by the CEM amounts to +42 mm (+8%) unaccounted for by climate and is subsequently assumed to represent the net positive contribution of watershed disturbance $\Delta -Q_{dist}$. The decrease in annual streamflow was –178 mm (–36%) relative to the 10-year reference period versus 201 mm (–39%) relative to the 5-year reference period, and lower precipitation was the dominant factor in both cases (Table 3 and Figure 7).

3.1.4 | WaSSI hydrologic simulation

The WaSSI simulated streamflow (Figure 8a) confirmed the declining trend in streamflow found in the attribution analysis. The found date

of April 1998 corroborates with the significant time interval found in the change point analysis.

3.2 | Arizona watershed

3.2.1 | Double-mass curves

Values of the F statistic were comparable with the SC values ($p < 10^{-6}$); however, here, the linear model coefficient (runoff coefficient) increased considerably, from 0.132 (5-year reference period) to 0.393 (Figure 6b), in response to the exceptionally wet period between November 2004 and February 2005 (80 to 165 mm/month). The increase in runoff coefficient with respect to the 10-year reference period was in the same order of magnitude. The effect of the

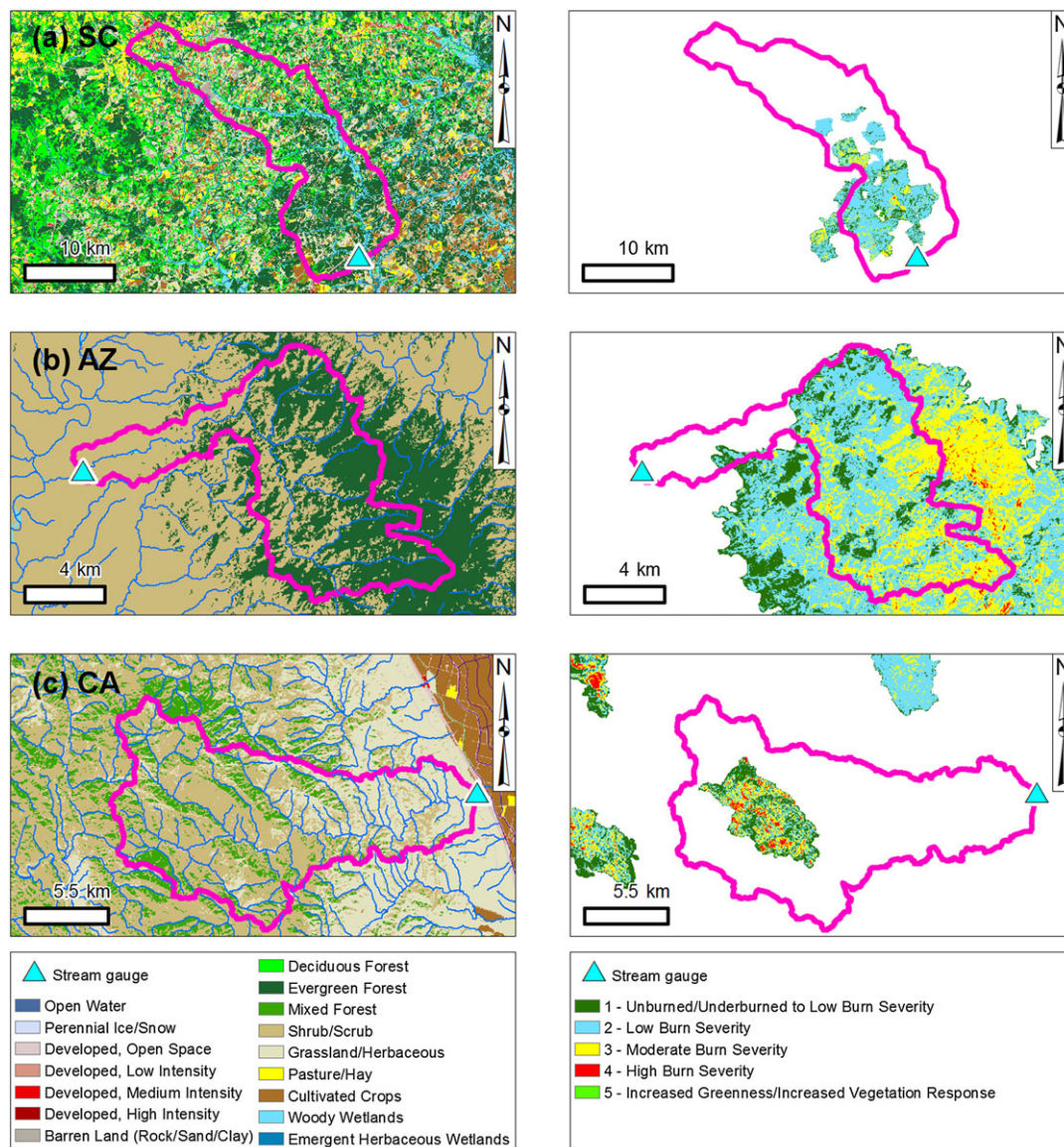


FIGURE 3 2001 Land cover (left panel) and burn severity (right panel) for the (a) Black Creek watershed (SC) with a series of 44 prescribed burns conducted between 2004 and 2013; (b) Wet Bottom Creek watershed (AZ) and the 2004 Willow Fire; and (c) Del Puerto Creek watershed (CA) and the 2003 Deer Park Fire (National Land Cover Database, 2011; Monitoring Trends in Burn Severity, 2014). Legends apply to all watersheds

wildfire was observed during the first winter, where the residual plot shows that runoff is nearly 400 mm more than expected. The runoff coefficient had not recovered to its pre-disturbance value 5 years after the fire in 2009, based on the increasing trend in the residual plot (Figure 6b), or even as late as 2012 verified with additional analysis.

3.2.2 | Attribution of streamflow changes (climate elasticity model)

The 5-year CEM₀ predicted an increase in streamflow of 24 mm (+47%) corresponding to an increase of precipitation from 437 to 507 mm. This predicted increase in streamflow fell short of the observed increase of +134 mm (+266%), with the difference (+110 mm or +219%) representing the effect of the 2004 Willow Fire in this watershed. Although fire disturbance is responsible for a considerable increase in runoff, the effect was amplified by increased precipitation (Table 3 and Figure 7a). Although the change in

streamflow was much smaller evaluated over a longer period, relative contributions (Table 3 and Figure 7b) of climate and fire disturbance were proportional to the changes observed relative to the 5-year reference period.

3.2.3 | WaSSI hydrologic simulation

The residual plot in Figure 8b (right panel) shows that the hydrological model reproduced the observed values correctly until the autumn of 2000 but was unable to simulate the intermittent character of streamflow after this date. While the dry winters were simulated correctly, the discrepancy was possibly related to low winter precipitation in 2003 and 2008, which represented a greater challenge for calculating water balances and led to an overestimation of the non-climate contribution to streamflow changes (Figure 8b, right panel). Nonetheless, the model simulated the dynamic of rapid increase in streamflow in November–December 2004 following the wildfire, while the

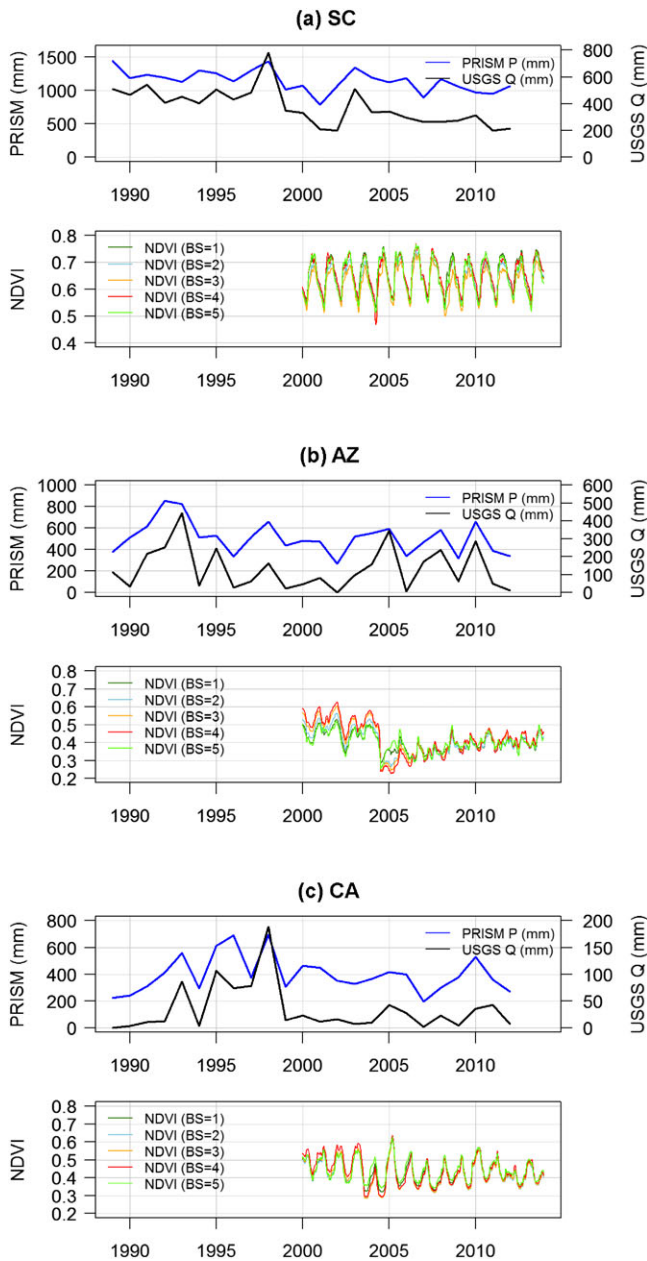


FIGURE 4 1981–2010 normal annual precipitation (PRISM), observed streamflow (USGS), and bi-weekly normalized difference vegetation index (NDVI) for MTBS burn severity classes (1—under/unburned to low, 2—low, 3—moderate, 4—high, 5—increased greenness) in the (a) Black Creek watershed (SC), (b) Wet Bottom Creek watershed (AZ), and (c) Del Puerto Creek (CA)

observed streamflow increased even more rapidly than before, providing minimal additional evidence of a non-climate contribution to streamflow change.

3.3 | California watershed

3.3.1 | Double-mass curves

There was a significant break point in the DMC corresponding with the July 2003 Deer Park wildfire ($p < 10^{-6}$), and the runoff coefficient increased from 0.04 (4%) to 0.058 (5.8%; Figure 6c, left panel). Unlike the AZ watershed, this increase was not observed until the second

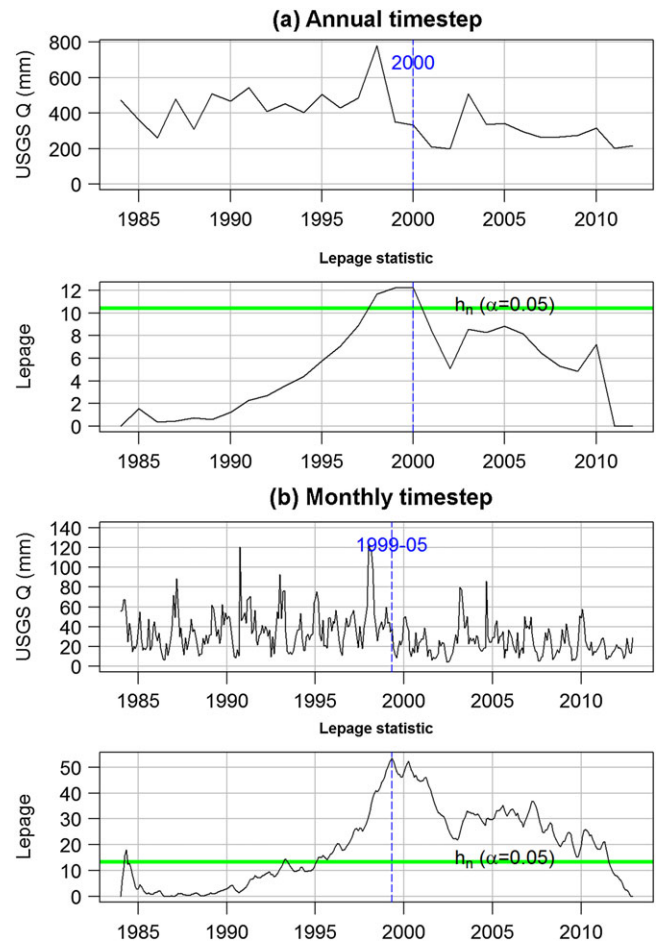


FIGURE 5 Change point analysis of the SC streamflow data for the period 1984–2012. Shown are the streamflow time series and Lepage test statistics evaluated for (a) annual time intervals and (b) monthly time intervals. The vertical dashed line indicates the estimated change point location corresponding with the greatest value of the Lepage statistic, and h_n marks the statistic value for a significance level of $\alpha = 0.05$

winter after the fire, in December 2004. The DMC for the 10-year reference period (Figure 6c, right panel) shows that there is a moment of even greater change in the DMC corresponding with the exceptionally high rainfall of 158 and 251 mm in January and February 1998, respectively.

3.3.2 | Attribution of streamflow changes (climate elasticity model)

Lower precipitation in the post-disturbance period (342 mm against 453 mm in the reference period) resulted in -33 mm (-64%) less streamflow. Judging from these numbers, it would be difficult to argue that the 2003 Deer Park Fire could have resulted in more runoff; however, CEM₀ predicted a much greater reduction of streamflow (-52 mm or -102%) than observed, meaning that fire disturbance itself increased the streamflow by +19 mm (+38%). The disturbance partly offset the effect of a declining annual precipitation on annual streamflow relative to the 5-year reference period (Figure 7a). When evaluated for the 10-year reference period, the CEM fitted to this period could explain all of the change in streamflow.

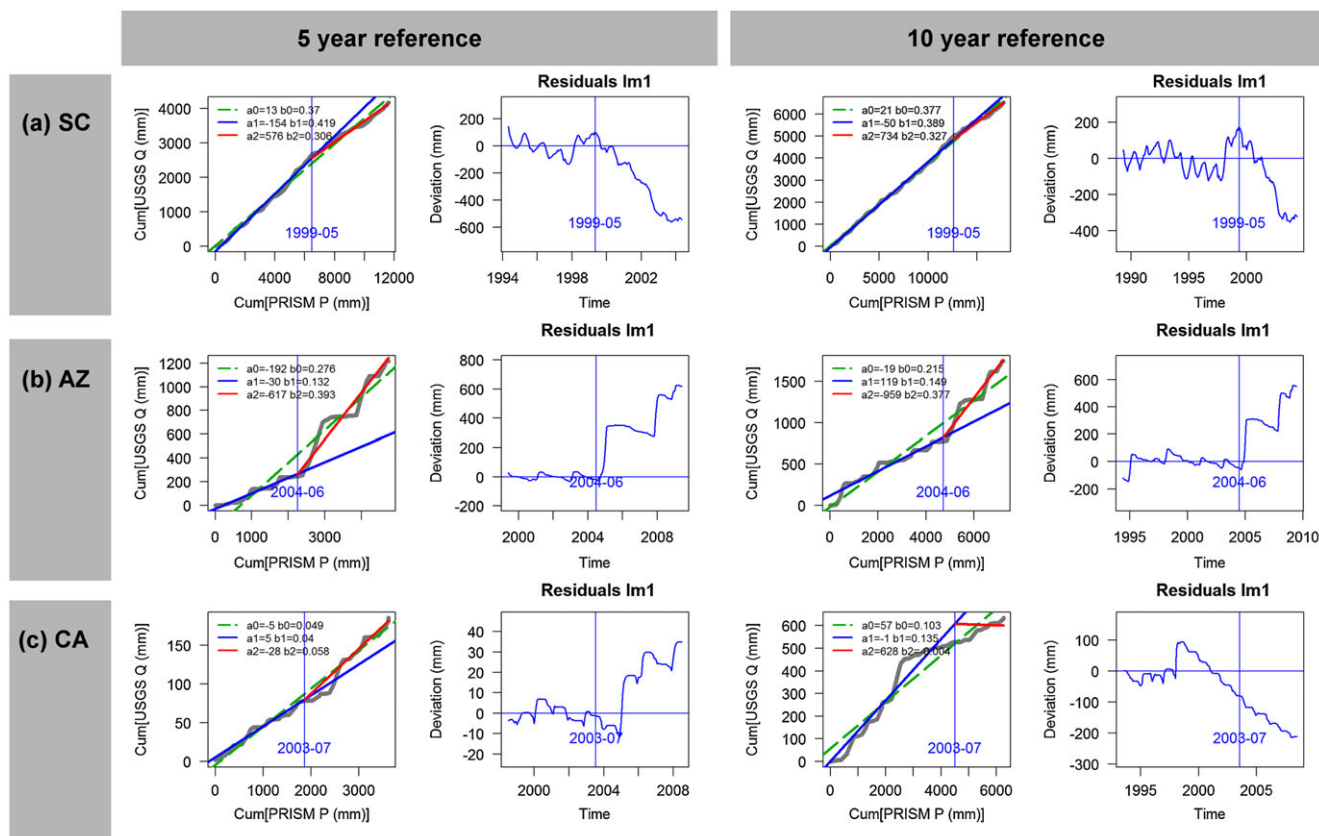


FIGURE 6 Double-mass and residual plots of monthly streamflow (USGS-GAGES-II) and monthly precipitation (PRISM) for the period that includes 5-year pre-disturbance and 5-year post-disturbance (left panel) and for the period that includes 10-year pre-disturbance and 5-year post-disturbance (right panel). The DMC based on the restricted linear model is represented by the orange dashed line, while the blue and red lines represent the DMC based on the unrestricted linear models fitted to the reference and post-disturbance periods, respectively. The residual plots show the deviations with respect to DMC fitted to the corresponding reference period

3.3.3 | WaSSI hydrologic simulation

The WaSSI simulation for this watershed was complicated by the systematic overestimation of summer and winter runoff, resulting in a propagated error in cumulative water yield (Figure 8c, center panel). Therefore, the WaSSI results for the CA watershed could not be interpreted for the purpose of disturbance analysis.

4 | DISCUSSION

The framework combines hydrological data and methods into a single procedure for the assessment of wildland fire impacts on water yields in single watersheds, and as such, presents a more practical assessment tool compared with traditional paired watershed analysis.

4.1 | Can the framework quantify wildland fire impacts on streamflow?

Yes, the framework uses CPM and DMC to detect changes in streamflow, and subsequently, a CEM to distinguish between the respective contributions of climate and wildland fire or other non-climate related disturbances to that streamflow change. CEM results can subsequently be compared with an attribution analysis based on WaSSI hydrologic simulations. If other non-climate disturbances

occurred than wildland fire alone, it is possible to estimate the relative impact of these disturbances using the CPM. As demonstrated for the three case studies, the contribution of fire disturbance to streamflow change can vary from negligible (SC) to substantial (AZ) or somewhere in between (CA).

Wildfire had an increasing effect on 5-year water yields in the AZ and CA watersheds; however, the net amount of change in streamflow and the direction of this change also depended on climate trends: an amplified response in conjunction with a positive trend in precipitation in the AZ watershed and an attenuated response in the CA watershed where post-wildfire precipitation was lower. The framework found an increase in runoff coefficient of the CA watershed from 4% to 5.8% despite a -64% lower yield that agrees with the steady baseflow observed throughout most of the winter in the post-fire period. The modest contribution of wildfire to streamflow change in the CA watershed was furthermore consistent with the rapid recovery of NDVI, and conversely, the slow recovery of NDVI in the AZ watershed agreed with the large contribution of wildfire to streamflow change there.

The CEM associated streamflow changes in the SC watershed mainly to climate rather than to fire. Climate was quite variable with a wet winter in 1998 (September 1997 to April 1998 were all months with >100 mm) followed by a period of less precipitation and lower mean annual number of extreme precipitation days >50.8 mm (see Appendix). The change point model linked the time of maximum

TABLE 3 Simulated contributions of climate change and (non-climate) watershed disturbance to changes in streamflow (mm/year) in the 5-year post-disturbance, including the year in which the disturbance occurred, versus the five preceding years and 10 preceding years, respectively. Climate elasticity models of changes in streamflow include a reduced model based on changes in precipitation (CEM₀) and a two-parameter climate elasticity model based on changes in precipitation and PET (CEM₁). Model selection was based on the lowest small-sample AIC (Sugiura, 1978; Hurvich & Tsai, 1991).

Watershed	Period	\bar{P}	\bar{PET}	\bar{Q}	ΔQ_0	CEM ₀ $\frac{dQ}{d\alpha} = \alpha \frac{dP}{d\alpha}$	CEM ₁ $\frac{dQ}{d\alpha} = \alpha \frac{dP}{d\alpha} + \beta \frac{dPET}{d\alpha}$	Model selection	$\Delta \bar{Q}_{clim}$	Attribution
Black Creek, South Carolina (SC)	1999–2003 (5-year post-disturbance)	1054	978	320						
	1994–1998 (5-year reference)	1283	964	521	201 (-39%)	$\alpha=2.62$ ($p=.08$) ($n=5$, $AIC_C=6.16$)	$\alpha=1.28$ ($p=.34$) $\beta=5.35$ ($p=.16$) ($n=5$, $AIC_C=22.35$)	CEM ₀	-242 (-47%)	+42 (+8%)
	1989–1998 (10-year reference)	1260	972	499	-178 (-36%)	$\alpha=1.54$ ($p=.04$) ($n=10$, $AIC_C=-2.45$)	$\alpha=1.68$ ($p=.008$) $\beta=3.48$ ($p=.02$) ($n=10$, $AIC_C=-5.34$)	CEM ₀	-125 (-25%)	-53 (-11%)
Wet Bottom Creek, Arizona (AZ)	2004–2008 (5-year post-disturbance)	507	863	184						
	1999–2003 (5-year reference)	437	904	50	+134 (+266%)	$\alpha=2.95$ ($p=.03$) ($n=5$, $AIC_C=14.56$)	$\alpha=2.77$ ($p=.05$) $\beta=9.21$ ($p=.30$) ($n=5$, $AIC_C=32.46$)	CEM ₀	+24 (+47%)	+110 (+219%)
	1994–2003 (10-year reference)	474	877	79	+105 (+133%)	$\alpha=2.76$ ($p=.03$) ($n=10$, $AIC_C=26.17$)	$\alpha=2.38$ ($p=.06$) $\beta=-5.91$ ($p=.34$) ($n=10$, $AIC_C=29.25$)	CEM ₀	+15 (+19%)	+89 (+114%)
Del Puerto Creek, California (CA)	2003–2007 (5-year post-disturbance)	342	902	18						
	1998–2002 (5-year reference)	453	866	51	-33 (-64%)	$\alpha=4.16$ ($p=.01$) ($n=5$, $AIC_C=18.65$)	$\alpha=3.19$ ($p=.02$) $\beta=-17.2$ ($p=.08$) ($n=5$, $AIC_C=32.84$)	CEM ₀	-52 (-102%)	+19 (+38%)
	1993–2002 (10-year ref.)	480	901	61	-42 (-70%)	$\alpha=2.42$ ($p=.004$) ($n=10$, $AIC_C=22.73$)	$\alpha=2.69$ ($p=.001$) $\beta=-6.63$ ($p=.08$) ($n=10$, $AIC_C=22.85$)	CEM ₀	-42 (-70%)	0 (0%)

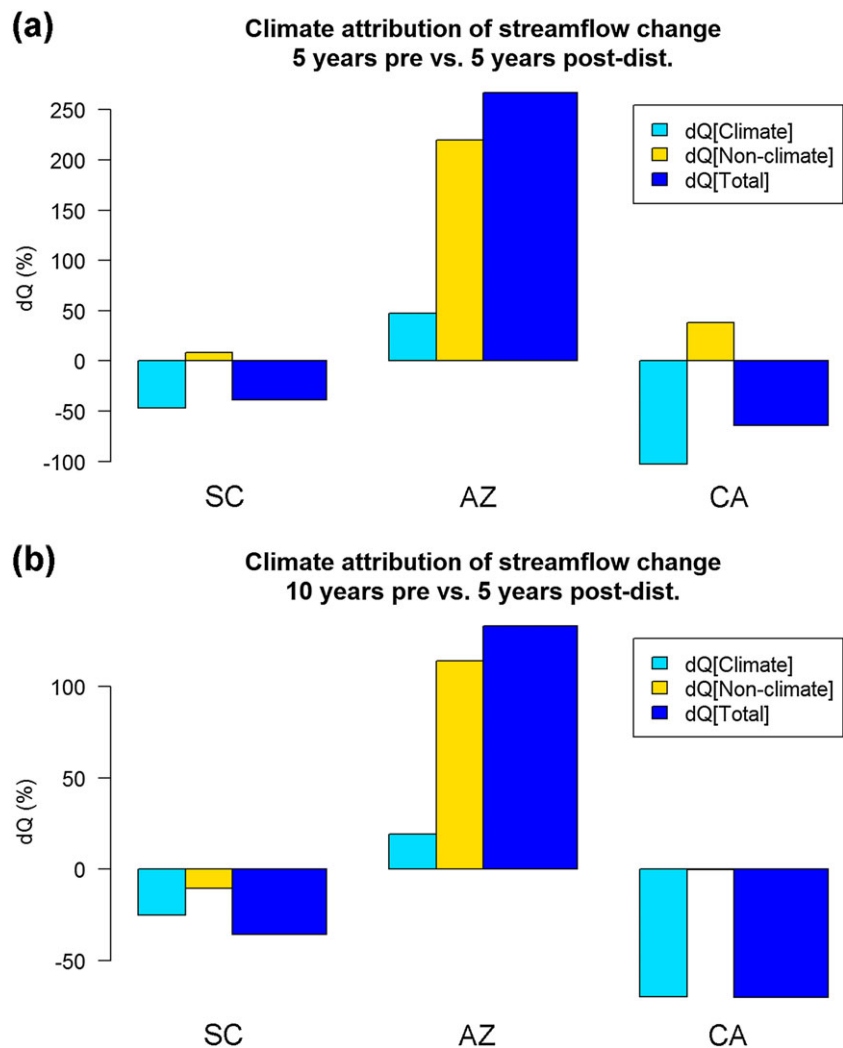


FIGURE 7 Attribution of the mean change in annual streamflow to climate variability (precipitation) and (non-climate) watershed disturbance, given in % change in the 5-year post-disturbance (including the year in which the disturbance occurred), versus the five preceding years (a) and 10 preceding years (b), respectively

streamflow disturbance (L_{max}) to May 1999, where the CEM attributed the observed loss in water yield of -39% to a negative (-47%) climate contribution attenuated by a positive ($+8\%$) non-climate contribution (5-year reference period). The change point analysis furthermore detected significant change in streamflow for the extended period between 1998 and 2000 (annual time step; Figure 5a) and 1995–2011 (monthly time step; Figure 5b), corresponding with periods of increased interannual and monthly variability in streamflow, respectively.

Although the framework was designed to quantify effects of climate trends and wildfire disturbance, other types of disturbance can also be identified when the approximate dates of disturbance found by the CPM can be linked to known events. The modest increase in streamflow in the SC watershed attributed to non-climate factors could not be linked with individual-prescribed fires, which agrees with earlier observations by Troendle, MacDonald, Luce, and Larsen (2010) that low severity prescribed fires are unlikely to influence water yield, especially compared with the effects of high severity wildfires. Estimates say that at least 20% of basal area of vegetation must be removed to cause any significant change in streamflow (Bosch & Hewlett, 1982; Stednick, 1996). Prescribed burnings followed a regular pattern (small fires with low burn severity; Carolina Sandhills NWR, 1998; 1999); no wildfires were reported, and bark beetle activity was

very low (Carolina Sandhills NWR, 1998; Carolina Sandhills NWR, 1999; South Carolina Forestry Commission, 1999). Therefore, the change in streamflow was possibly the result of a combination of dam failure (Carolina Sandhills NWR, 1994; 1999), beaver activity (Carolina Sandhills NWR, 1999), major weather events (severe thunderstorm on May 6, 1999 that killed many trees; National Climatic Data Center Storm Events Database, retrieved February 8, 2016; and an ice and snowstorm on January 24–25, 2000; Carolina Sandhills NWR, 2000), or (unverified) water management and water usage.

4.2 | Does the framework account for overlapping watershed disturbances?

The framework can separate climate effects overlapping with non-climate effects; however, multiple overlapping non-climate disturbances are sometimes difficult to disentangle. This is the case for the CA watershed, where the DMC has no clear break point for the 2006 Canyon Fire even though it burned an area similar in size to the 2003 Del Puerto Creek Fire. Hydrologic responses to overlapping watershed disturbances are furthermore complicated by the interaction with extreme climate events and the gradual recovery of vegetation and evapotranspiration. Also, not all break points in the DMC correspond with non-climate disturbance. For example, the 10-year reference

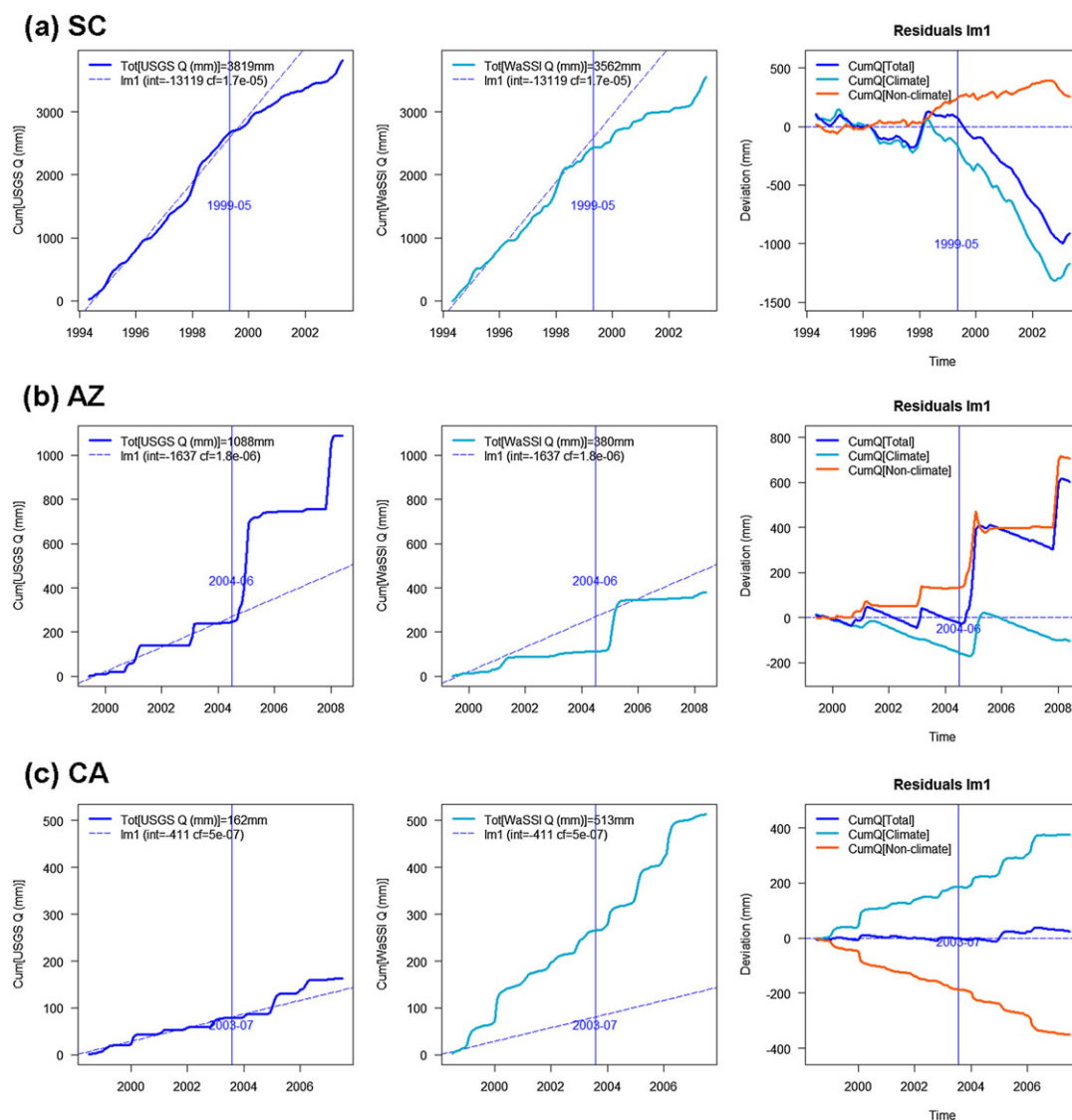


FIGURE 8 Cumulative contributions of climate variability on streamflow simulated in WaSSI and (non-climate) watershed disturbance calculated as the difference between observed and simulated cumulative streamflow

period preceding the 2003 wildfire in the CA watershed includes both the strong El Niño year 1997–1998 with exceptionally high rainfall and the drier La Niña years 1998–1999 and 1999–2000, where the 5-year reference period included only the La Niña years. El Niño effects are strong in this part of California (Hoell et al., 2016), and the high precipitation during 1997–1998 phase may have resulted in erosion and alteration of the streambed, causing a break point in the DMC (Figure 6c).

With a larger sample size and wider range of annual precipitation and runoff, a 10-year reference period will generally provide more robust estimates of CEM coefficients than the a 5-year reference period (see also Figure 4c). Nevertheless, this does not imply that the 10-year CEM improves the accuracy of the attribution analysis for individual wildfires because, in the case of the CA watershed, there was another smaller fire (1996) in this period. The length of the evaluated reference and post-disturbance periods is a trade-off between the amount of hydrological data needed to construct a CEM on one hand and the likelihood of overlapping disturbance effects on the other hand. Choosing an appropriate length is very challenging in California

watersheds where high fire frequency meets extreme climate and ephemeral runoff, and in this case, the true wildfire effect on runoff may lie somewhere between the values attributed using the 5-year and 10-year reference periods, respectively. It will be useful to evaluate whether the inclusion of antecedent climate conditions (temperature days, precipitation, and snow water equivalents) and monthly variance of high resolution precipitation data (Hao et al., 2015) improves the CEM. Linking hydrologic disturbance directly to burn severity or MODIS NDVI may also help validate the attribution analysis, although the more complex disturbance patterns may necessitate a distributed ecological-hydrological model.

4.3 | Which climates work best with the framework?

The accuracy of the attribution analysis depends on the performance of models in the framework and may be considered acceptable for temperate, humid, and Mediterranean climates provided that annual water yield efficiencies (runoff coefficients) are approximately constant during the pre-disturbance and post-disturbance periods,

respectively. The precipitation-only based CEMs with the best performance in terms of AIC_c (low value reflecting the greatest maximum likelihood for n observations) were obtained for the SC watershed (Table 3), with values of $AIC_c = 6.16$ (5-year reference) and $AIC_c = -2.45$ (10-year reference). This is explained by the stable annual water yield (of 33%) and perennial streamflow resulting from year-round precipitation, which can be accurately represented in a linear CEM. CEM performance for the AZ and CA watersheds was lower (greater AIC_c values) because of a greater seasonal and interannual variability in the precipitation–streamflow relationship associated with snowmelt (AZ) and El Niño effects (CA). Notwithstanding, snow is the dominant hydrologic input in much of the western United States (Rocky Mountains, Sierra Nevada, and Cascade Ranges), and therefore, snow processes (annual snowfall, snowmelt, and sublimation) are important controlling factors of streamflow disturbance in this area (Troendle & King, 1985; Harpold et al., 2014). Long-term and short-term drought is common in regions like Southern California, Nevada, and other parts of the Southwest, where it represents a contributing factor to wildfire and affects streamflow (Littell, Peterson, Riley, Liu, & Luce, 2016). Hydrologic response to wildfire is highly nonlinear in snow-dominated, arid, or drought-affected systems, and under such conditions, the framework would benefit from a more physically based nonlinear CEM.

4.4 | What are some limitations of the framework?

Other limitations are related to the way in which the attribution analysis identifies disturbance effects. Fire impacts vary with burn severity, which affects the amount of leaf area reduction. High burn severity reduces evapotranspiration drastically, increases net precipitation, and leaves the soil exposed to direct rainfall impact (Winkler et al., 2010). Post-fire soil surface sealing and heat-induced soil water repellency change the amount of runoff generated along the hillslope (Larsen et al., 2009; Ebel, Moody, & Martin, 2012), while the spatial sequence of burned areas controls how much of the generated runoff is transported downhill (Moody et al., 2016). Storm flow studies emphasize the importance of the organization of flow paths on the timing of flow delivery at the base of the hillslope (Hallema & Moussa, 2014; Hallema, Moussa, Sun, & McNulty, 2016) and the watershed (Hallema, Moussa, Andrieux, & Voltz, 2013); however, the framework lumps all these effects together. This eliminates the possibility to evaluate wildland fire impacts on individual hydrological processes (e.g., infiltration and storm flow generation) but also creates the possibility to evaluate wildland fire effects on a much wider range of watersheds.

4.5 | Why not use either change point model or double-mass curve to evaluate disturbances instead of both?

The CPM and DMC were used to evaluate slightly different types of disturbances and are complementary tools in the framework. The CPM was used to detect observed changes in streamflow, while the DMC was used to evaluate changes in water yield efficiency (streamflow expected based on precipitation). This is necessary because wildfire and precipitation trends can partly cancel each other

out (CA watershed) in which case streamflow data alone may not be sufficient to find the timing of the disturbance. On the other hand, the CPM can detect multiple disturbances (with the Lepage test), where the classic DMC approach evaluates only one disturbance at a time (F test). Therefore, the inclusion of both CPM and DMC offers the best chances of finding all significant disturbances. The disadvantage of CPM is that the Lepage statistic for intermittent or ephemeral streamflow series will rarely be significant ($L > h_t$ given α) if there are many months out of the year with zero flow.

5 | CONCLUSIONS

A framework was presented for the assessment of wildland fire impacts on annual water yields in watersheds. This framework uses a change point model to identify and assess multiple disturbances where existing and a climate elasticity model to determine the contributions of climate variability and wildland fire to streamflow changes over a multiyear period. Case studies showed that the framework can detect delayed hydrological responses to wildfire and establish whether wildfire enhanced or attenuated streamflow regardless of precipitation trends during the period of evaluation (AZ and CA watersheds). In the third case study (SC watershed), change in streamflow could not be linked to prescribed fire but was chiefly attributed to a declining trend in precipitation.

Based on the outcomes, we conclude that the framework has a potential to capture the streamflow impacts of wildfires, prescribed fires, and various other watershed disturbances under a variety of watershed characteristics (mountainous and mixed land cover) and climate conditions (humid and Mediterranean/temperate). The framework is a step-up from traditional analyses because it can be used with long-term streamflow data from a single-flow station and does not rely on paired watershed data. Furthermore, if there is more than one potential disturbance event, the change point model can indicate the relative impact of each disturbance, making the framework suitable for a wide range of applications including hydrologic impact assessment of wildland fires, erosion modeling, and post-fire management. The challenge in the future development of the framework lies in the adaptation and proper representation of seasonal and interannual variability in the precipitation–streamflow relationship in the CEM for a wider range of conditions, including snowfall/snowmelt patterns, seasonal drought, and multiyear drought.

ACKNOWLEDGEMENTS

The authors want to thank William M. Christie (USDA Forest Service) for processing NDVI and aerial detection survey data and John G. Cobb (USDA Forest Service) for his assistance with database development. We further acknowledge Dr Danny C. Lee and the two anonymous reviewers, whose comments and suggestions have been extremely valuable in revising the manuscript. Financial support for this study was provided by the U.S. Department of Agriculture Forest Service Southern Research Station, the Joint Fire Science Program (project #14-1-06-18), and the U.S. Forest Service Research Participation Program administered by the Oak Ridge Institute for Science and Education through an interagency agreement between the U.S.

Department of Energy and the USDA Forest Service. ORISE is managed by Oak Ridge Associated Universities (ORAU) under DOE contract number DE-AC05-06OR23100. All opinions expressed in this paper are the authors' and do not necessarily reflect the policies and views of USDA, DOE, or ORAU/ORISE.

REFERENCES

- Akaike, H. (1973). Information theory and an extension of the maximum likelihood principle. In B. N. Petrov, & F. Csaki (Eds.), *2nd international symposium on information theory*. (pp. 267–281). Budapest: Akademia Kiado.
- Anderson, H. W. (1955). Detecting hydrologic effects of changes in watershed conditions by double-mass analysis. *Eos, Transactions American Geophysical Union*, *36*(1), 119–125.
- Bart, R. R. (2016). A regional estimate of post-fire streamflow change in California. *Water Resources Research*, *52*, 1465–1478. doi:10.1002/2014WR016553
- Biederman, J. A., Somor, A. J., Harpold, A. A., Gutmann, E. D., Breshears, D. D., Troch, P. A., ... Brook, P. D. (2015). Recent tree die-off has little effect on streamflow in contrast to expected increases from historical studies. *Water Resources Research*, *51*(12), 9775–9789. doi:10.1002/2015WR017401
- Bladon, K. D., Emelko, M. B., Silins, U., & Stone, M. (2014). Wildfire and the future of water supply. *Environmental Science & Technology*, *48*, 8936–8943. doi:10.1021/es500130g
- Bosch, J. M., & Hewlett, J. D. (1982). A review of catchment experiments to determine the effect of vegetation changes on water yield and evapotranspiration. *Journal of Hydrology*, *55*, 3–23.
- Bowman, D. M. J. S., O'Brien, J. A., & Goldammer, J. G. (2013). Pyrogeography and the global quest for sustainable fire management. *Annual Review of Environment and Resources*, *38*, 57–80. doi:10.1146/annurev-environ-082212-134049
- Brown, T. C., Hobbins, M. T., & Ramirez, J. A. (2008). Spatial distribution of water supply in the conterminous United States. *Journal of the American Water Resources Association*, *44*(6), 1474–1487. doi:10.1111/j.1752-1688.2008.00252.x
- Burnash, R. J. C. (1995). The NWS river forecast system—catchment modeling. In V. P. Singh (Ed.), *Computer models of watershed hydrology*. (pp. 311–366). Littleton, Colorado: Water Resources Publications.
- Burnash, R. J. C., Ferral, R. L., & McGuire, R. A. (1973). A generalized streamflow simulation system—conceptual modeling for digital computers. Technical Report. Joint Federal and State River Forecast Center, US National Weather Service and California Department of Water Resources, Sacramento, California204.
- Caldwell, P. V., Sun, G., McNulty, S. G., Cohen, E. C., & Moore Myers, J. A. (2011). Modeling impacts of environmental change on ecosystem services across the conterminous United States. In C. N. Medley, G. Patterson, & M. J. Parker (Eds.), *Observing, studying, and managing for change: Proceedings of the Fourth Interagency Conference on Research in the Watersheds: U.S. Geological Survey Scientific Investigations Report 2011:5169*, 202 p.
- Caldwell, P. V., Sun, G., McNulty, S. G., Cohen, E. C., & Moore Myers, J. A. (2012). Impacts of impervious cover, water withdrawals, and climate change on river flows in the conterminous US. *Hydrology and Earth System Sciences*, *16*, 2839–2285. doi:10.5194/hess-16-2839-2012
- Caldwell, P. V., Miniati, C. F., Elliott, K. J., Swank, W. T., Brantley, S. T., & Laseter, S. H. (2016). Declining water yield from forested mountain watersheds in response to climate change and forest mesophication. *Global Change Biology*, *22*, 2997–3012. doi:10.1111/gcb.13309
- Carolina Sandhills National Wildlife Refuge. Annual narrative report: Calendar year 1994. US Fish and Wildlife Service, Department of the Interior, 36 p.
- Carolina Sandhills National Wildlife Refuge. Annual narrative report: Calendar year 1999. US Fish and Wildlife Service, Department of the Interior, 38 p.
- Carolina Sandhills National Wildlife Refuge. Annual narrative report: Calendar year 2000. US Fish and Wildlife Service, Department of the Interior, 42 p.
- Chow, G. C. (1960). Tests of equality between sets of coefficients in two linear regressions. *Econometrica: Journal of the Econometric Society*, 591–605.
- Clark, K. L., Skowronski, N., Gallagher, M., Renninger, H., & Schäfer, K. (2012). Effects on invasive insects and fire on forest energy exchange and evapotranspiration in the New Jersey pinelands. *Agricultural and Forest Meteorology*, 166–167, 50–61. doi:10.1016/j.agrformet.2012.07.007
- Daly, C., Neilson, R. P., & Phillips, D. L. (1994). A statistical-topographic model for mapping climatological precipitation over mountainous terrain. *Journal of Applied Meteorology*, *33*, 140–158.
- Daly, C., Gibson, W. P., Taylor, G. H., Johnson, G. L., & Pasteris, P. (2002). A knowledge-based approach to the statistical mapping of climate. *Climate Research*, *22*, 99–113.
- Danielson JJ, Gesch, DB. 2011. Global multi-resolution terrain elevation data 2010 (GMTED2010). U.S. Geological Survey Open-File Report 2011–1073, 26 p.
- DeBano, L. F. (2000). The role of fire and soil heating on water repellency in wildland environments: A review. *Journal of Hydrology*, 231–232, 195–206. doi:10.1016/S0022-1694(00)00194-3
- Dennison, P. E., Brewer, S. C., Arnold, J. D., & Moritz, M. A. (2014). Large wildfire trends in the western United States, 1984–2011. *Geophysical Research Letters*, *41*, 2928–2933. doi:10.1002/2014GL059576
- Ebel, B. A., Moody, J. A., & Martin, D. A. (2012). Hydrologic conditions controlling runoff generation immediately after wildfire. *Water Resources Research*, *48*, W03529. doi:10.1029/2011WR011470
- Eidenshink, J., Schwind, B., Brewer, K., Zhu, Z. L., Quayle, B., & Howard, S. (2007). A project for monitoring trends in burn severity. *Fire Ecology*, *3*(1), 3–21. doi:10.4996/FIREECOLOGY.0301003
- Fisher, F. M. (1970). Tests of equality between sets of coefficients in two linear regressions: An expository note. *Econometrica*, *38*(2), 361–366. doi:10.2307/1913018
- Foster, H. A. (1934). Duration curves. *Transactions of the American Society of Civil Engineers*, *99*(1), 1213–1235.
- Fu, G., Charles, S. P., & Chiew, F. H. S. (2007). A two-parameter climate elasticity of streamflow index to assess climate change effects on annual streamflow. *Water Resources Research*, *43*, W11419. doi:10.1029/2007WR005890
- Glenn-Lewin, D. C., Peet, R. K., & Veblen, T. T. (Eds) (1992). *Plant succession: Theory and prediction* (Vol. 11). London: Chapman and Hall.
- Godfrey B. 1999. Koppen climate classification for the conterminous United States. Idaho State Climate Services, Moscow, Idaho. Retrieved from: <https://catalog.data.gov/dataset/koppen-climate-classification-for-the-conterminous-united-states>, Accessed April 02, 2016.
- Hallema, D. W., & Moussa, R. (2014). A model for distributed GIUH-based flow routing on natural and anthropogenic hillslopes. *Hydrological Processes*, *28*, 4877–4895. doi:10.1002/hyp.9984
- Hallema, D. W., Moussa, R., Andrieux, P., & Voltz, M. (2013). Parameterization and multi-criteria calibration of a distributed storm flow model applied to a Mediterranean agricultural catchment. *Hydrological Processes*, *27*, 1379–1398. doi:10.1002/hyp.9268
- Hallema DW, Moussa R, Sun G, McNulty SM. (2016). Surface storm flow prediction on hillslopes based on topography and hydrologic connectivity. *Ecological Processes*, (in press).
- Hamon, W. R. (1961). Estimating potential evapotranspiration. *Journal of the Hydraulics Division*, *87*, 107–120.
- Hao, L., Sun, G., Liu, Y., Wan, J., Qin, M., Qian, H., ... Chen, J. (2015). Urbanization dramatically altered the water balances of a paddy field-dominated basin in southern China. *Hydrology and Earth System Sciences*, *19*, 3319–3331. doi:10.5194/hess-19-3319-2015
- Harpold, A. A., Biederman, J. A., Condon, K., Merino, M., Korgaonkar, Y., Nan, T., ... Brooks, P. D. (2014). Changes in snow accumulation and

- ablation following the Las Conchas Forest Fire, New Mexico, USA. *Ecohydrology*, 7, 440–452. doi:10.1002/eco.1363
- Hart, S. J., Schoennagel, T., Veblen, T. T., & Chapman, T. B. (2015). Area burned in the western United States is unaffected by recent mountain pine beetle outbreaks. *Proceedings of the National Academy of Sciences*, 112(14), 4375–4380. doi:10.1073/pnas.1424037112
- Hawkins, D. M., & Zamba, K. D. (2005). A change-point model for a shift in variance. *Journal of Quality Technology*, 37(1), 21–31.
- Hawkins, D. M., Qiu, P. H., & Kang, C. W. (2003). The changepoint model for statistical process control. *Journal of Quality Technology*, 35(4), 355–366.
- Helvey, J. D. (1980). Effects of a north central Washington wildfire on runoff and sediment production. *Water Resources Bulletin*, 16(4), 627–634.
- Helvey, J. D., & Patric, J. H. (1965). Canopy and litter interception of rainfall by hardwoods of eastern United States. *Water Resources Research*, 1(2), 193–206.
- Hirakawa, K. (1974). The comparison of powers of distribution-free two-sample test. *TRU Mathematics*, 10, 65–82.
- Hoell, A., Hoerling, M., Eischeid, J., Wolter, K., Dole, R., Perlwitz, J., ... Cheng, L. (2016). Does El Niño intensity matter for California precipitation? *Geophysical Research Letters*, 43, 819–825. doi:10.1002/2015GL067102
- Homer, C. G., Dewitz, J. A., Yang, L., Jin, S., Danielson, P., Xian, G., ... Megown, K. (2015). Completion of the 2011 National Land Cover Database for the conterminous United States—representing a decade of land cover change information. *Photogrammetric Engineering and Remote Sensing*, 81(5), 345–354.
- Huang, F., Xia, Z., Guo, L., & Yang, F. (2014). Effects of reservoirs on seasonal discharge of Irtysh River measured by Lepage test. *Water Science and Engineering*, 7(4), 363–372. doi:10.3882/j.issn.1674-2370.2014.04.002
- Hurvich, C. M., & Tsai, C.-L. (1991). Bias of the corrected AIC criterion for underfitted regression and time series models. *Biometrika*, 78, 499–509.
- Inoue, T., & Matsumoto, J. (2007). Abrupt climate changes observed in late August over Central Japan between 1983 and 1984. *Journal of Climate*, 20, 4957–4967. doi:10.1175/JCLI4217.1
- Jung, H. Y., Hogue, T. S., Rademacher, L. K., & Meixner, T. (2009). Impact of wildfire on source water contributions in Devil Creek, CA: Evidence from end-member mixing analysis. *Hydrological Processes*, 23(2), 183–200. doi:10.1002/hyp.7132
- Karl, T. R., Knight, R. W., & Plummer, N. (1995). Trends in high-frequency climate variability in the twentieth century. *Nature*, 377, 217–220.
- Kenny, J. F., & Juracek, K. E. (2012). Description of 2005–10 domestic water use for selected U.S. cities and guidance for estimating domestic water use: U.S. Geological Survey Scientific Investigations Report 2012–5163, 31 p.
- Key, C. H., & Benson, N. C. (2006). Landscape assessment: Sampling and analysis methods. In D. C. Lutes, R. E. Keane, J. F. Caratti, C. H. Key, N. C. Benson, S. Sutherland, & L. J. Gangi (Eds.), *FIREMON: Fire effects*.
- Kottek, M., Grieser, J., Beck, C., Rudolf, B., & Rubel, F. (2006). World map of the Köppen-Geiger climate classification update. *Meteorologische Zeitschrift*, 15(3), 259–263.
- Krawchuk, M. A., & Moritz, M. A. (2014). Burning issues: Statistical analyses of global fire data to inform assessments of environmental change. *Environmetrics*, 25, 472–481. doi:10.1002/env.2287
- Larsen, I. J., MacDonald, L. H., Brown, E., Rough, D., Welsh, M. J., Pietraszek, J. H., ... Shaffrath, K. (2009). Causes of post-fire runoff and erosion: Water repellency, cover, or soil sealing. *Soil Science Society of America Journal*, 73, 1393–1407. doi:10.2136/sssaj2007.0432
- Leake, S. A., & Pool, D. R. (2010). Simulated effects of groundwater pumping and artificial recharge on surface-water resources and riparian vegetation in the Verde Valley sub-basin, Central Arizona: U.S. Geological Survey Scientific Investigations Report 2010-5147, 18 p.
- Lepage, Y. (1971). Combination of Wilcoxon and Ansari-Bradley Statistics. *Biometrika*, 58, 213–217.
- Littell, J. S., Peterson, D. L., Riley, K. L., Liu, Y., & Luce, C. H. (2016). A review of the relationships between drought and forest fire in the United States. *Global Change Biology*, 22(7), 2353–2369. doi:10.1111/gcb.13275
- Lloyd, C. E. M., Freer, J. E., Collins, A. L., Johnes, P. J., & Jones, J. I. (2014). Methods for detecting change in hydrochemical time series in response to targeted pollutant mitigation in river catchments. *Journal of Hydrology*, 514, 297–312. doi:10.1016/j.jhydrol.2014.04.036
- Martin, D. (2016). At the nexus of fire, water and society. *Philosophical Transactions of the Royal Society B*, 371. doi:10.1098/rstb.2015.0172.20150172
- Matlock, M., Thoma, G., Cummings, E., Cothren, J., Leh, M., & Wilson, J. (2013). Geospatial analysis of potential water use, water stress, and eutrophication impacts from US dairy production. *International Dairy Journal*, 31, S78–S90. doi:10.1016/j.dairyj.2012.05.001
- Matsuyama, H., Marengo, J. A., Obregon, G. O., & Nobre, C. A. (2002). Spatial and temporal variabilities of rainfall in tropical South America as derived from climate prediction center merged analysis of precipitation. *International Journal of Climatology*, 22, 175–195. doi:10.1002/joc.724
- Merriam, C. F. (1937). Comprehensive study of the rainfall on the Susquehanna Valley. *Transactions of the American Geophysical Union*, pt. 2471–476.
- Miller, J. D., & Thode, A. E. (2007). Quantifying burn severity in a heterogeneous landscape with a relative version of the delta normalized burn ratio (dNBR). *Remote Sensing of Environment*, 109, 66–80.
- Monitoring Trends in Burn Severity Data Access: Fire level geospatial data. MTBS Project (USDA Forest Service/U.S. Geological Survey). Retrieved from: <http://mtbs.gov>, accessed 01/11/2014
- Mood, A. (1954). On the asymptotic efficiency of certain nonparametric two-sample tests. *Annals of Mathematical Statistics*, 25, 514–533.
- Moody, J. A., Ebel, B. A., Nyman, P., Martin, D. A., Stoof, C. R., & McKinley, R. (2016). Relations between soil hydraulic properties and burn severity. *International Journal of Wildland Fire*, 25, 279–293. doi:10.1071/WF14062
- National Climatic Data Center Storm Events Database, 2016. Retrieved from: <http://www.ncdc.noaa.gov/stormevents/eventdetails.jsp?id=5691456>, Accessed August 02, 2016
- National Research Council (2008). *Hydrologic effects of a changing forest landscape*. Washington, DC: National Academies Press.
- Natural Resources Conservation Service, 2012. United States Department of Agriculture, US General Soil Map (STATSGO2). Retrieved from: <https://catalog.data.gov/dataset/statsgo>
- Neary DG, Ryan KC, DeBano, LF, eds. 2005. *Wildland fire in ecosystems: Effects of fire on soil and water*. Gen. Tech. Rep. RMRS-GTR-32-vol. 4. Ogden, UT: U.S. Department of Agriculture, Forest Service, Rocky Mountain Research Station, 250 p.
- R Core Team. 2014. R: A language and environment for statistical computing. R Foundation for Statistical Computing, Vienna, Austria. Retrieved from <http://www.R-project.org/>
- Renniger, H. J., Clark, K. L., Skowronski, N., & Schäfer, K. V. R. (2013). Effects of a prescribed fire on water use and photosynthetic capacity of pitch pines. *Trees*, 27, 1115–1127. doi:10.1007/s00468-013-0861-5
- Ross, G. J. (2015). Parametric and nonparametric sequential change detection in R: The cpm package. *Journal of Statistical Software*, 66(3).
- Ross, G. J., Tasoulis, D. K., & Adams, N. M. (2011). Nonparametric monitoring of data streams for changes in location and scale. *Technometrics*, 53(4), 379–389. doi:10.1198/TECH.2011.10069
- Sankarasubramanian, A., Vogel, R. M., & Limbrunner, J. F. (2001). Climate elasticity of streamflow in the United States. *Water Resources Research*, 37(6), 1771–1781. doi:10.1029/2000WR900330
- Schaake, J. C. (1990). In P. E. Waggoner (Ed.), chap. 8 *From climate to flow, in climate change and U.S. water resources*. (pp. 177–206). New York: John Wiley.

- Searcy, J.K., Hardison, C.H. 1960. Double-mass curves. Manual of hydrology: Part I. General surface-water techniques. U.S. Geological Survey Water-Supply Paper 1541-B.
- Shakesby, R. A., & Doerr, S. H. (2006). Wildfire as a hydrological and geomorphological agent. *Earth-Science Reviews*, 74, 269–307. doi:10.1016/j.earscirev.2005.10.006
- Sillins, U., Bladon, K. D., Kelly, E. N., Esch, E., Spence, J. R., Stone, M., ... Tichkowsky, I. (2014). Five-year legacy of wildfire and salvage logging impacts on nutrient runoff and aquatic plant, invertebrate, and fish productivity. *Ecohydrology*, 7(6), 1508–1523. doi:10.1002/eco.1474
- South Carolina Forestry Commission. 1998. Annual report July 1, 1997 – June 30, 1998. Retrieved from: <http://www.state.sc.us/forest/ar98.htm> Accessed on February 8, 2016.
- South Carolina Forestry Commission. 1999. Annual report July 1, 1998 – June 30, 1999. Retrieved from: <http://www.state.sc.us/forest/ar99.htm> Accessed on February 8, 2016.
- Spatial Climate Analysis Service. 2004. Oregon State University. Retrieved from: <http://www.prism.oregonstate.edu>, accessed 01/02/2015
- Stednick, J. D. (1996). Monitoring the effects of timber harvest on annual water yield. *Journal of Hydrology*, 176, 79–95.
- Sugiura, N. (1978). Further analysis of the data by Akaike's information criterion and the finite corrections. *Communications in statistics: Theory and methods*, A7, 13–26.
- Sun, G., McNulty, S. G., Moore-Myers, J. A., & Cohen, E. C. (2008). Impacts of multiple stresses on water demand and supply across the southeastern United States. *Journal of the American Water Resources Association*, 44, 1441–1457. doi:10.1111/j.1752-1688.2008.00250.x
- Sun, G., Caldwell, P., Noormets, A., Cohen, E., McNulty, S., Treasure, E., ... Chen, J. (2011). Upscaling key ecosystem functions across the conterminous United States by a water-centric ecosystem model. *Journal of Geophysical Research*, 116, G00J05.
- Sun, S., Sun, G., Caldwell, P. V., McNulty, S. G., Cohen, E. C., Xiao, J., & Zhang, Y. (2015a). Drought impacts on ecosystem functions of the U. S. National Forests and Grasslands: Part I evaluation of a water and carbon balance model. *Forest Ecology and Management*, 353, 260–268.
- Sun, G., Caldwell, P. V., & McNulty, S. G. (2015b). Modelling the potential role of forest thinning in maintaining water supplies under a changing climate across the conterminous United States. *Hydrological Processes*, 29, 5016–5030. doi:10.1002/hyp.10469
- Temperli, C., Bugmann, H., & Elkin, C. (2013). Cross-scale interactions among bark beetles, climate change, and wind disturbances: A landscape modeling approach. *Ecological Monographs*, 83, 383–402. doi:10.1890/12-1503.1
- Thornton, P. E., Thornton, M. M., Mayer, B. W., Wilhelmi, N., Wei, Y., Devarakonda, R., & Cook, R. B. (2014). Daymet: Daily surface weather data on a 1-km grid for North America, version 2. Data set. Retrieved from: <http://daac.ornl.gov> from Oak Ridge National Laboratory Distributed Active Archive Center, Oak Ridge, Tennessee, USA. Accessed July 01, 2015. doi:10.3334/ORNLDAAC/1219
- Troendle, C. A., & Bevenger, G. S. (1996). Effect of fire on streamflow and sediment transport, Shoshone National Forest, Wyoming. In Proceedings of the Second Biennial Conference on the Greater Yellowstone Ecosystem, The Ecological Implications of Fire in Greater Yellowstone, September 19–21, 1993, Yellowstone National Park, Wyoming, Greenlee J (ed.). International Association of Wildland Fire: Fairfield, WA43–52.
- Troendle, C. A., & King, R. M. (1985). The effect of timber harvest on the Fool Creek Watershed, 30 years later. *Water Resources Research*, 21(12), 1915–1922. doi:10.1029/WR021i012p01915
- Troendle, C. A., MacDonald, L. H., Luce, C. H., & Larsen, I. J. (2010). Fuel management and water yield. Chapter 7. In W. J. Elliot, I. S. Miller, & L. Audin (Eds.), *2010 Cumulative watershed effects of fuel management in the western United States. Gen. Tech. Rep. RMRS-GTR-231*. (pp. 299). Fort Collins, CO: U.S. Department of Agriculture, Forest Service, Rocky Mountain Research Station.
- U.S. Geological Survey, 2015. National Water Information System data available on the World Wide Web (USGS Water Data for the Nation). Retrieved from: <http://waterdata.usgs.gov/nwis/>, accessed 01/12/2015
- Vivès B, Jones RN. 2005. Detection of abrupt changes in Australian decadal rainfall. CSIRO Atmospheric Research Technical Paper 73, p.27.
- Vogel, R. M., & Fennessey, N. M. (1994). Flow-duration curves. I: New interpretation and confidence intervals. *Journal of Water Resources Planning and Management*, 120(4), 485–504.
- Wang, H., Chen, L., & Yu, X. (2016). Distinguishing human and climate influences on streamflow changes in the Luan River basin in China. *Catena*, 136, 182–188. doi:10.1016/j.catena.2015.02.013
- Wei, X., & Zhang, M. (2010). Quantifying streamflow change caused by forest disturbance at a large spatial scale: A single watershed study. *Water Resources Research*, 46, W12525. doi:10.1029/2010WR009250
- Winkler, R. D., Moore, R. D., Redding, T. E., Spittlehouse, D. L., Smerdon, B. D., & Carlyle-Moses, D. E. (2010). The effects of forest disturbance on hydrologic processes and watershed response. In: Pike RG, Redding TE, Moore RD, Winker RD, Bladon KD (eds), 2010. Compendium of forest hydrology and geomorphology in British Columbia. B.C. Min. For. Range, For. Sci. Prog., Victoria, B.C. and FORREX Forum for Research and Extension in Natural Resources, Kamloops, B.C. Land. *Managers Handbook*, 66.
- Yang, T., Chen, X., Xu, C.-Y., & Zhang, Z.-C. (2009). Spatio-temporal changes of hydrological processes and underlying driving forces in the Guizhou region, southwest China. *Stochastic Environmental Research and Risk Assessment*, 23, 1071–1087. doi:10.1007/s00477-008-0278-7
- Yue, S., & Wang, C. (2002). The influence of serial correlation on the Mann-Whitney test for detecting a shift in median. *Advances in Water Resources*, 25(3), 325–333. doi:10.1016/S0309-1708(01)00049-5
- Zhang, M., & Wei, X. (2012). The effects of cumulative forest disturbance on streamflow in a large watershed in the central interior of British Columbia, Canada. *Hydrology and Earth System Sciences*, 16, 2021–2034. doi:10.5194/hess-16-2021-2012

How to cite this article: Hallema DW, Sun G, Caldwell PV, et al. Assessment of wildland fire impacts on watershed annual water yield: Analytical framework and case studies in the United States. *Ecohydrology*. 2017;10:e1794. <https://doi.org/10.1002/eco.1794>

APPENDIX

Methods and statistics

Mann-Whitney statistic

The Mann-Whitney statistic is defined as (e.g., Yue & Wang, 2002; Ross et al., 2011)

$$U = \min\{U_S, U_T\}, \quad (7)$$

$$U_S = n_S n_T + \frac{n_S(n_S + 1)}{2} - r(x_i) \quad (8)$$

$$U_T = n_S n_T + \frac{n_T(n_T + 1)}{2} - r(x_i) \quad (9)$$

where the subscripts *S* and *T* correspond to the sets of observations preceding and following the presumed change point τ , respectively, *n* is the corresponding number of observations, and $r(x_i)$ represents the pooled rank sums given all observations.

Mood statistic

The Mood statistic M is given by (Mood, 1954; Ross et al., 2011)

$$M = \left| \left(M' - \mu_{M'} \right) / \sigma_{M'} \right| \quad (10)$$

where

$$M' = \sum_{x_i \in S} (r(x_i) - (n+1)/2)^2 \quad (11)$$

$$\mu_{M'} = \frac{n_S(n^2-1)}{12}, \quad (12)$$

$$\sigma_{M'}^2 = n_S n_T (n+1)(n^2-4)/180 \quad (13)$$

where $\mu_{M'}$ and $\sigma_{M'}^2$ are the mean and variance of the Mood statistic, respectively.

Precipitation duration (PDC) and flow duration (FDC)

The FDC is the complement of the cumulative distribution of streamflow that shows the percentage time of a given streamflow was equaled or exceeded during the period of evaluation. This percentage represents the probability of exceedance p of a given discharge Q , where p is defined by (Foster, 1934; Vogel & Fennessey, 1994)

$$p = 1 - P\{Q \leq q\} \quad (14)$$

Each set of climate and watershed characteristics yields a unique FDC and typically contains a fast flow component and a delayed flow component. The FDC changes as a result of climate variability and/or watershed characteristics, and for this reason, provides an important indicator for watershed disturbance. The precipitation duration curve (PDF) was found by substituting streamflow in Equation 7 with precipitation.

Break point detection in DMC with the Chow test

The first step in detecting a break point in the DMC was to calculate the cumulative streamflow and precipitation for the reference and post-disturbance cumulative data. Next, we determined the DMC by fitting two separate linear models (the unrestricted models) to the reference and post-disturbance periods and estimated the cumulative runoff as follows:

$$Q_{cum,1} = a_1 + b_1 \cdot P_{cum,1} + \varepsilon_1 \quad (15)$$

$$Q_{cum,2} = a_2 + b_2 \cdot P_{cum,2} + \varepsilon_2, \quad (16)$$

where the subscripts 1 and 2 correspond with the reference and post-disturbance periods, respectively, parameters a and b were fitted using the least squares method, and ε represents the residual error. Note that in order to obtain a continuous unrestricted DMC, the linear model for the post-disturbance period was forced through the break point approximated by the model for the reference period.

The following step was to fit the restricted linear model to the pooled data for both periods. This restricted model was defined as follows:

$$Q_{cum,0} = a_0 + b_0 \cdot P_{cum,0} + \varepsilon_0. \quad (17)$$

If there is no break point in the DMC it follows that

$$H_0 : a_1 = a_2, b_1 = b_2. \quad (18)$$

This was evaluated by testing whether the differences in sums of squared residuals from the unrestricted model and the restricted model were statistically significant using the Chow test (Chow, 1960; Fisher, 1970).

The Chow statistic was calculated as follows (Chow, 1960; Fisher, 1970):

$$F = \frac{\{SSE_0 - (SSE_1 + SSE_2)\} / K}{(SSE_1 + SSE_2) / (n-2K)}, \quad (19)$$

with SSE_0 as the sum of squared errors for the restricted linear model representing the DMC for the pooled data, SSE_1 and SSE_2 as the sum of squared errors for the unrestricted linear models for the reference and post-disturbance periods, respectively, K as the number of regressors and n as the number of samples.

Corrected Akaike's information criterion

The corrected (small sample) Akaike's information criterion (AIC_c) was calculated as follows (Sugiura, 1978; Hurvich & Tsai, 1991):

$$AIC_c = -2L_k + 2k + \frac{2k(k+1)}{n-k-1}, \quad (20)$$

where n is the number of observations, L_k is the maximized log-likelihood, and k is the number of parameters in the climate elasticity model. The AIC_c is based on Akaike's information criterion (Akaike, 1973) and imposes a greater penalty for extra parameters, thus decreasing the probability of overfitting the climate elasticity model as a result of adding too many parameters.

Precipitation duration and flow duration curves

South Carolina watershed

Mean annual precipitation in the SC watershed was lower in the post-disturbance period (Table 3), and the number of precipitation days ($p\{P_d \geq 1 \text{ mm}\}$) decreased from 113 to 101 days/year on average (exceedance $p = .31$ and $p = .28$, respectively; left panel in Figure 9a). Consequently, the 75th percentile of daily flow Q_d decreased from 6.0 to 3.6 m^3/s (Figure 9a, right panel). Mean annual number of extreme precipitation days $>50.8 \text{ mm}$ also decreased, from 1.6 days ($p\{P_d \geq 50.8 \text{ mm}\} = 0.0044$) to 0.6 days ($p\{P_d \geq 50.8 \text{ mm}\} = 0.0016$), while the 10th percentile discharge exceedance decreased from 9.1 to 5.4 m^3/s .

Arizona watershed

Precipitation in the AZ watershed increased from 437 to 507 mm in the post-disturbance period (Table 3), and the mean annual number of precipitation days likewise increased from 45 days

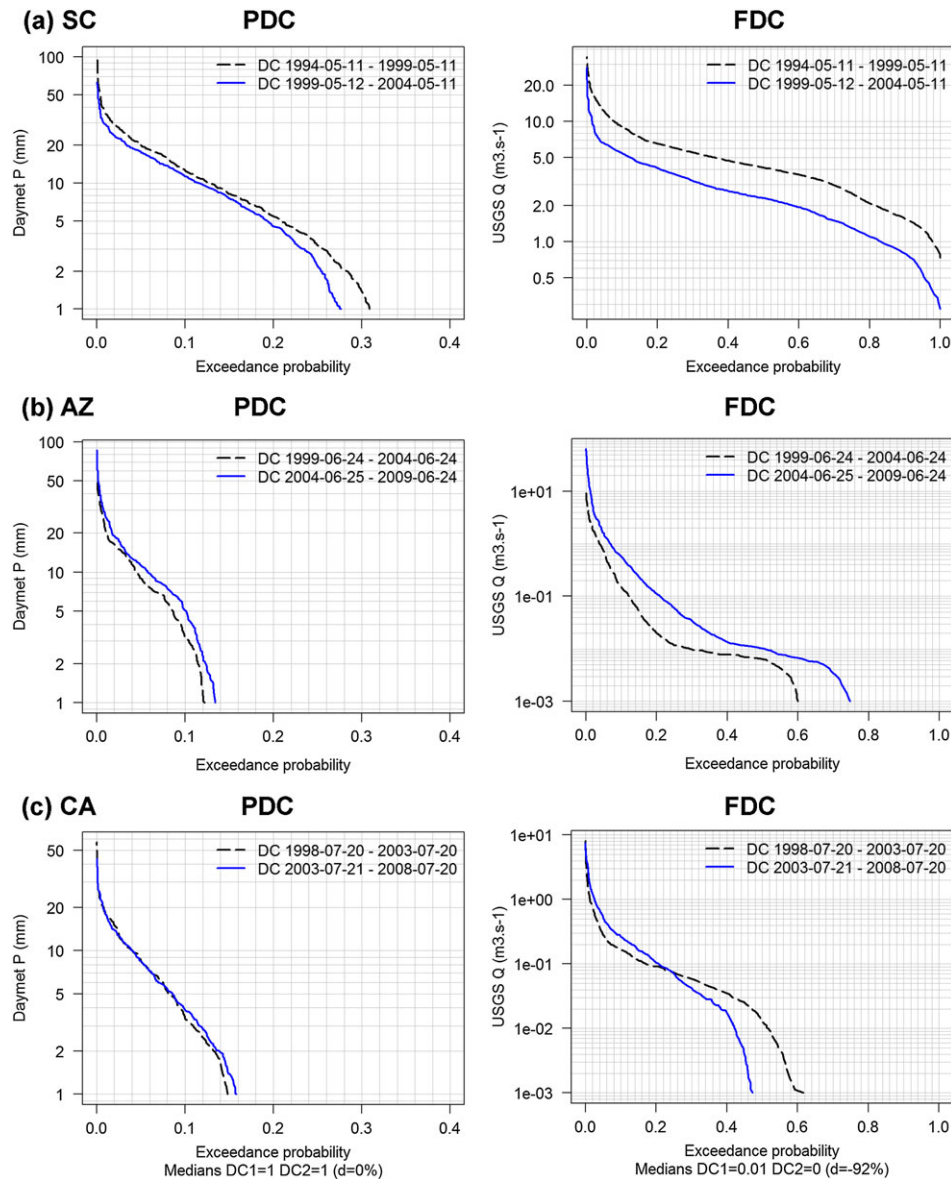


FIGURE 9 Precipitation duration curves (PDCs) based on Daymet daily precipitation data aggregated to the watershed scale for the 5-year periods before (dashed) and after disturbance and corresponding flow duration curves (FDC) based on daily USGS GAGES-II streamflow data

($p\{P_d \geq 1 \text{ mm}\} = 0.122$) to 49 days ($p\{P_d \geq 1 \text{ mm}\} = 0.134$; Figure 9b, left panel). Mean annual number of days with streamflow increased considerably from to 219 days ($p\{Q_d \geq 1.0 \times 10^{-3} \text{ m}^3/\text{s}\} = 0.600$) to 272 days ($p\{Q_d \geq 1.0 \times 10^{-3} \text{ m}^3/\text{s}\} = 0.746$), and the 10th percentile discharge exceedance is more than tripled (0.50 v. 0.15 m^3/s) (Figure 9b, right). These high flows occurred mostly in the winter when the mean annual snow water equivalent varied between 8 mm (November) and 110 mm (January) (reference and post-disturbance period combined), and high daily maximum temperatures (12°C during the coldest month of January) allowed for immediate snowmelt.

California watershed

The CA watershed received less precipitation during the post-disturbance period, 342 mm compared with 453 mm in the reference period

(Table 3). The mean annual number of precipitation days increased from 54 days ($p\{P_d \geq 1 \text{ mm}\} = 0.158$) in the reference period to 58 days ($p\{P_d \geq 1 \text{ mm}\} = 0.148$) in the post-disturbance period, while the number of days with moderate precipitation did not change substantially (1.2 days [$p\{P_d \geq 25.4 \text{ mm}\} = 0.003$] v. 1.0 days [$p\{P_d \geq 25.4 \text{ mm}\} = 0.0027$], see Figure 9c, left). Heavy precipitation $\geq 50.8 \text{ mm}$ was observed only once, during the reference period. Despite the minor change in precipitation duration and the 75th percentile of streamflow (from $7.4 \times 10^{-2} \text{ m}^3/\text{s}$ to $7.1 \times 10^{-2} \text{ m}^3/\text{s}$), flow variability increased substantially. The 10th percentile discharge exceedance increased by +59% from 0.17 to 0.27 m^3/s , while the number of days with streamflow dropped from 275 days ($p\{Q_d \geq 1.0 \times 10^{-3} \text{ m}^3/\text{s}\} = 0.616$) to 172 days ($p\{Q_d \geq 1.0 \times 10^{-3} \text{ m}^3/\text{s}\} = 0.472$; Figure 9c, right).